Article

Cell Reports

ATM and ATR Signaling Regulate the Recruitment of Human Telomerase to Telomeres

Graphical Abstract

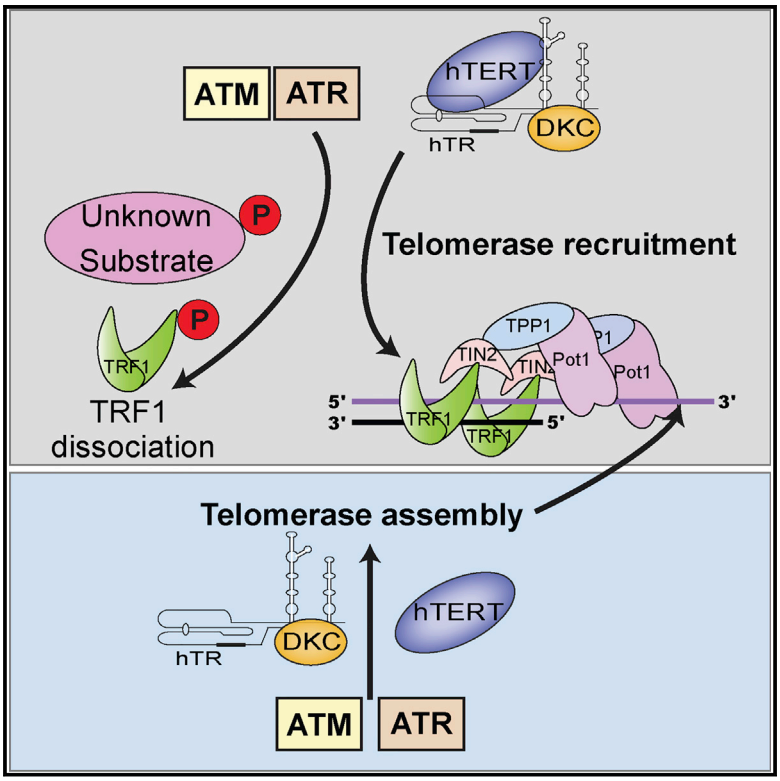

Highlights

- ATM and ATR are required for telomerase recruitment to telomeres in human cells
- Replication fork stalling triggers ATR-dependent telomerase recruitment to telomeres
- Phosphorylation of TRF1 at an SQ site contributes to telomerase recruitment
- ATM is required for telomere elongation in vivo

Authors

Adrian S. Tong, J. Lewis Stern, Agnel Sfeir, Melissa Kartawinata, Titia de Lange, Xu-Dong Zhu, Tracy M. Bryan

Correspondence

tbryan@cmri.org.au

In Brief

Tong et al. demonstrate that the DNA damage response kinases ATM and ATR are required for the presence of telomerase at telomeres in human cells. Replication fork stalling triggers ATR-mediated telomerase recruitment, and phosphorylation of the telomere-binding protein TRF1 at serine 367 also regulates the presence of telomerase at telomeres.

Tong et al., 2015, Cell Reports *13*, 1633–1646
November 24, 2015 ©2015 The Authors
http://dx.doi.org/10.1016/j.celrep.2015.10.041

Cell Reports
Article

ATM and ATR Signaling Regulate the Recruitment of Human Telomerase to Telomeres

Adrian S. Tong,[1,6] J. Lewis Stern,[1,4,6] Agnel Sfeir,[2,5] Melissa Kartawinata,[1] Titia de Lange,[2] Xu-Dong Zhu,[3] and Tracy M. Bryan[1,*]
[1]Cell Biology Unit, Children's Medical Research Institute, University of Sydney, Westmead, NSW 2145, Australia
[2]Laboratory for Cell Biology and Genetics, The Rockefeller University, New York, NY 10065, USA
[3]Department of Biology, McMaster University, Hamilton, ON L8S 4K1, Canada
[4]Present address: Department of Chemistry and Biochemistry, University of Colorado, Boulder, CO 80309, USA
[5]Present address: Skirball Institute of Biomolecular Medicine, Department of Cell Biology, NYU School of Medicine, New York, NY 10016, USA
[6]Co-first author
*Correspondence: tbryan@cmri.org.au
http://dx.doi.org/10.1016/j.celrep.2015.10.041

SUMMARY

The yeast homologs of the ATM and ATR DNA damage response kinases play key roles in telomerase-mediated telomere maintenance, but the role of ATM/ATR in the mammalian telomerase pathway has been less clear. Here, we demonstrate the requirement for ATM and ATR in the localization of telomerase to telomeres and telomere elongation in immortal human cells. Stalled replication forks increased telomerase recruitment in an ATR-dependent manner. Furthermore, increased telomerase recruitment was observed upon phosphorylation of the shelterin component TRF1 at an ATM/ATR target site (S367). This phosphorylation leads to loss of TRF1 from telomeres and may therefore increase replication fork stalling. ATM and ATR depletion reduced assembly of the telomerase complex, and ATM was required for telomere elongation in cells expressing POT1ΔOB, an allele of POT1 that disrupts telomere-length homeostasis. These data establish that human telomerase recruitment and telomere elongation are modulated by DNA-damage-transducing kinases.

INTRODUCTION

Vertebrate telomeres are repetitive TTAGGG DNA sequences located at the ends of chromosomes, which protect the coding regions of DNA. In mammalian germline cells and ~85% of cancers, telomere length is maintained by the dimeric ribonucleoprotein telomerase, which catalyzes the addition of TTAGGG repeats to counteract telomere shortening and cellular senescence (Shay and Bacchetti, 1997; Kim et al., 1994; Wenz et al., 2001). The minimal catalytic core of human telomerase consists of the telomerase reverse transcriptase protein (hTERT), telomerase RNA (hTR), and the protein dyskerin (Cohen et al., 2007).

The differentiation of telomeres from broken chromosome ends is conferred by a family of six telomere-specific binding proteins collectively termed "shelterin" (de Lange, 2005). This complex consists of the double-stranded binding proteins TRF1 and TRF2, the single-stranded binding proteins POT1 and TPP1, the bridging protein TIN2 that links these two groups of proteins, and Rap1 (reviewed in Palm and de Lange, 2008). TRF1 protects the telomere and negatively regulates telomerase-mediated telomere lengthening (van Steensel and de Lange, 1997; Smogorzewska et al., 2000; Ancelin et al., 2002; Karlseder et al., 2002). TRF1 also facilitates the progression of the replication machinery; deletion of TRF1 increases replication fork stalling, leading to ATR kinase activation and a "fragile telomere" phenotype (Sfeir et al., 2009; Martínez et al., 2009). The TRF1-mediated repression of the ATR response requires recruitment of the shelterin components TIN2 and the TPP1/POT1 heterodimer (Zimmermann et al., 2014).

TPP1 and POT1 also have roles in mediating telomere-length regulation. A surface on the N-terminal oligonucleotide/oligosaccharide-binding (OB) domain of TPP1 termed the TEL patch activates telomerase by stimulating telomerase processivity and providing a direct binding site for telomerase recruitment to telomeres; mutation of the TEL patch can lead to telomere shortening syndromes characterized by bone marrow failure (Abreu et al., 2010; Nandakumar et al., 2012; Zhong et al., 2012; Kocak et al., 2014; Guo et al., 2014; Dalby et al., 2015). Additionally, mutation analyses at sites independent of the TEL patch have implicated TPP1 as part of a telomere-length-dependent feedback loop that regulates telomere-length homeostasis (Sexton et al., 2014). A mutant form of POT1 that abrogates binding to single-stranded DNA (POT1ΔOB) deregulated telomere-length control (Loayza and De Lange, 2003), indicating that the DNA-binding capability of POT1 is vital as a negative regulator of telomere length. The impact of human POT1 on telomere length is complex, since both depletion and overexpression of POT1 lead to telomere lengthening (Ye et al., 2004; Veldman et al., 2004; Colgin et al., 2003; Armbruster et al., 2004). POT1 function as a positive or negative regulator of telomerase activity at the telomere depends on its position of binding relative to the DNA 3′ end

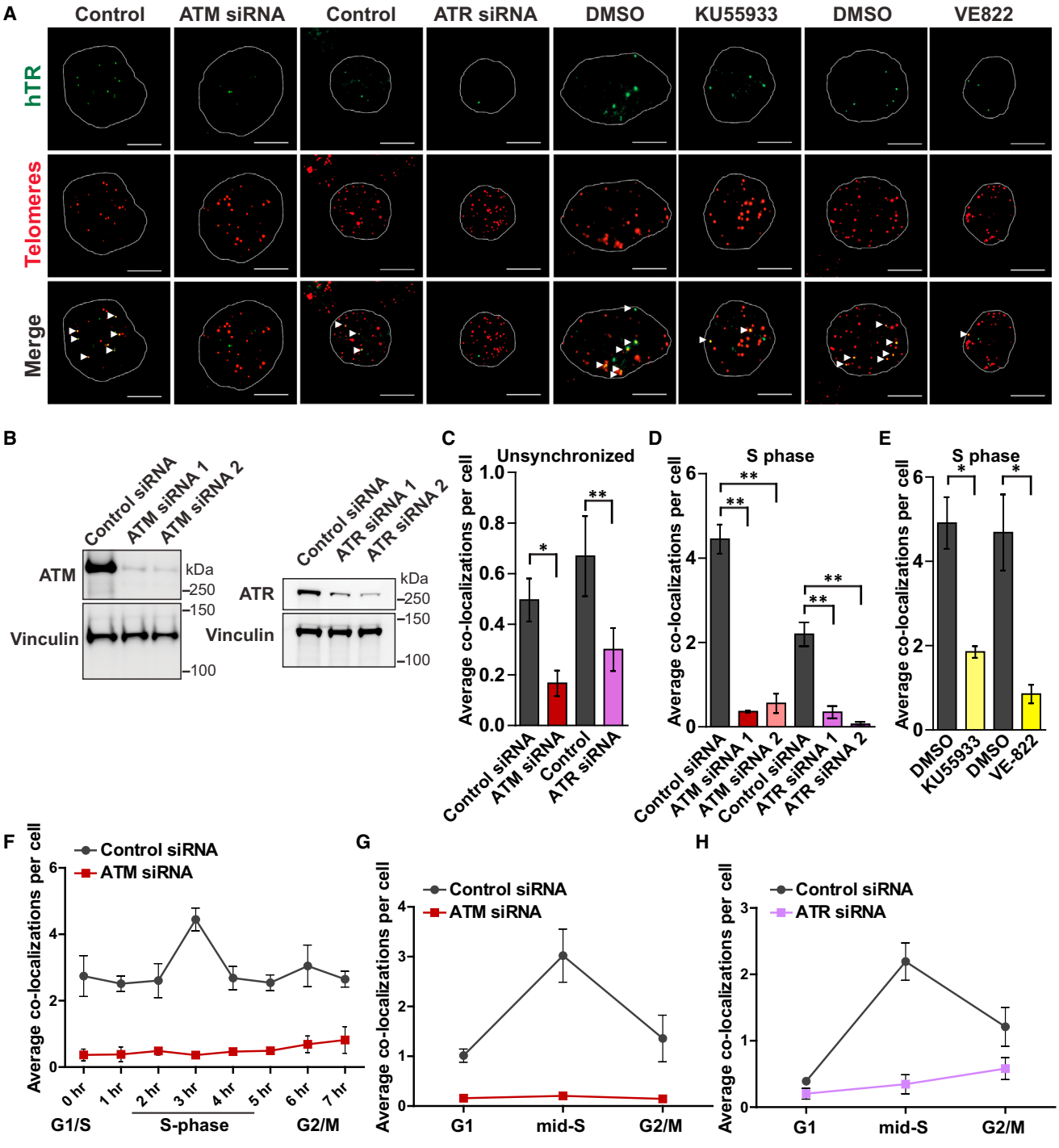

Figure 1. ATM and ATR Are Both Required for the Presence of Human Telomerase at Telomeres

(A) Representative images of hTR/telomere FISH in 293T cells treated with the indicated siRNAs or kinase inhibitors. Cells were synchronized to mid-S phase of the cell cycle and probed with hTR probes (green) or a telomere probe (red). Co-localizations are indicated by white arrows in the merge row. Scale bar, 10 μm.

(B) Immunoblot of 293T cells with either ATM (left panel) or ATR (right panel) siRNA-mediated knockdown, using the respective antibodies, with vinculin as a control.

(C) Average co-localizations between telomerase and telomeres in unsynchronized 293T cells treated with control siRNA (gray), ATM siRNA (red) (*p = 0.012), or ATR siRNA (purple) (**p = 0.0095).

(D) Quantitation of decrease in telomerase recruitment in S phase synchronized 293T cells following treatment with two independent ATM and ATR siRNAs; **p < 0.01. Cells were synchronized with a thymidine/aphidicolin block (ATM) or sorted into cell-cycle phases by FACS based on DNA content (ATR).

(legend continued on next page)

and is also modulated by its binding partner, TPP1 (Zaug et al., 2005; Wang et al., 2007; Lei et al., 2005; Kelleher et al., 2005).

Telomerase action at the telomere is highly regulated; it preferentially elongates the shortest telomeres, and recruitment of the enzyme complex to the telomere occurs in mid-S phase of the cell cycle (Bianchi and Shore, 2007; Britt-Compton et al., 2009; Teixeira et al., 2004; Hemann et al., 2001; Tomlinson et al., 2006; Jády et al., 2006). In both budding and fission yeasts, the preference of telomerase to extend the shortest telomeres requires the activity of Tel1, the yeast homolog of human ATM (Sabourin et al., 2007; Hector et al., 2007; Arnerić and Lingner, 2007). ATM and ATR are kinases within the phosphatidylinositol-3 kinase-related kinase (PIKK) family, which regulates cellular responses to DNA damage, mRNA decay, and nutrient-dependent signaling (Lovejoy and Cortez, 2009). Activation of these DNA damage pathways is dampened at telomeres; in mammalian cells, TRF2 represses activation of ATM while POT1 represses ATR (Karlseder et al., 2004; Celli and de Lange, 2005; Denchi and de Lange, 2007; Guo et al., 2007; Okamoto et al., 2013). Nevertheless, there is a large amount of evidence that their yeast homologs play a positive role in facilitating telomere extension by telomerase (Moser et al., 2009, 2011; Yamazaki et al., 2012; Churikov et al., 2013).

It is not known whether the role of the ATM and ATR pathways in recruiting telomerase is conserved in mammals. Although ATM deficiency or ATR mutations can induce telomere shortening or instability in human and mouse cells (Metcalfe et al., 1996; Smilenov et al., 1997; Wong et al., 2003; Wu et al., 2007; Pennarun et al., 2010), these kinases were reported to be dispensable for elongation of the shortest telomeres in mouse models (Feldser et al., 2006; McNees et al., 2010). Also, immortalized cell lines from human patients with ATM mutations are able to maintain their telomeres with telomerase, albeit at short lengths (Sprung et al., 1997). Nonetheless, there is evidence that TRF1-mediated telomere-length regulation in human cells involves ATM. Inhibition of human ATM resulted in increased TRF1 at the telomere, and phosphorylation of TRF1 on serine 367, an ATM/ATR target site, reduced the interaction of TRF1 with telomeres and abrogated its ability to inhibit telomere lengthening (McKerlie et al., 2012; Wu et al., 2007).

In this study, we report that both ATM and ATR are required for the recruitment of human telomerase to telomeres.

RESULTS

ATM and ATR Are Both Required for the Presence of Human Telomerase at Telomeres

We used fluorescence in situ hybridization (FISH) to detect human telomerase RNA (hTR) in combination with a probe for telomeres to visualize the presence of endogenous telomerase at telomeres in HEK293T cells (Stern et al., 2012) (Figure 1A). Depletion of ATM and ATR using small interfering RNA (siRNA) resulted in reduction of levels of each protein by ~95% and ~80%, respectively (Figure 1B), without causing significant perturbations in progression of the cells through the cell cycle (Figure S1A). Depletion of either kinase resulted in a significant decrease in telomerase recruitment to telomeres in asynchronously growing cells (Figures 1A and 1C). The roles of both ATM and ATR in telomerase recruitment were confirmed with a second siRNA against each protein (Figure 1D).

The involvement of the kinase activities of both ATM and ATR were demonstrated by using the kinase inhibitors KU-55933 and VE-822 (Figures 1A and 1E) at concentrations sufficient to inhibit ATM autophosphorylation and ATR activation, respectively (Figure S1B), without inhibiting related kinases (1.5 μM for KU-55933 and 0.5 μM for VE-822; Hickson et al., 2004; Fokas et al., 2014).

Telomerase recruitment across the cell cycle was examined by synchronizing cells at the G1/S boundary with overnight thymidine and aphidicolin treatments, followed by release from the cell-cycle block and harvest at hourly intervals (Figure S1A). Telomerase presence at the telomere peaks in mid-S phase (Figure 1F), as previously described (Tomlinson et al., 2006; Jády et al., 2006). Depletion of ATM abolished recruitment of telomerase to the telomere across all phases of the cell cycle (Figures 1F and S1C). Since this synchronization procedure is likely to cause DNA damage, we confirmed these observations by sorting ATM- and ATR-depleted cells by flow-activated cell sorting (FACS) into different cell-cycle phases based on DNA content (Figure S1A). Despite reduced numbers of hTR-telomere foci in control cells across the cell cycle (discussed further below), lack of either kinase again resulted in a large decrease in telomerase recruitment, particularly in S phase (Figures 1G and 1H). Reduction of hTR-telomere colocalizations across the cell cycle after ATM depletion was also demonstrated in a second human cell line, HeLa (Figures S1D–S1G). These results provide direct evidence that telomere shortening in telomerase-positive human cells defective in ATM and ATR activity is at least partially the result of diminished recruitment of telomerase to telomeres.

ATM Effect on Telomerase Recruitment Is Partially Mediated by TRF1

It is known that TRF1 is a substrate of ATM and/or other PIKK kinases, and such phosphorylation events lead to changes in TRF1 localization and telomere length (Kishi et al., 2001; Wu et al., 2007; McKerlie et al., 2012). To investigate whether these changes in telomere length are due to changes in the presence of telomerase at telomeres, we knocked down TRF1 by

(E) Average telomerase co-localization with telomeres in S phase synchronized 293T cells after treatment with DMSO vehicle (gray), 1.5 μM KU-55933 (light yellow), or 500 nM VE-822 (dark yellow); *$p < 0.05$.

(F) Telomerase co-localization with telomeres in 293T cells at the indicated number of hours after release from a thymidine/aphidicolin block, treated with control (gray) or ATM (red) siRNA.

(G) Telomerase co-localization with telomeres in 293T cells treated with control (gray) or ATM (red) siRNA. Cells were stained with the DNA dye VyBrant DyeCycle Violet and isolated into cell-cycle phases with FACS. Enrichment of cells in the indicated phases was confirmed by flow cytometry of sorted cells (Figure S1A).

(H) Telomerase co-localization with telomeres in 293T cells treated with control (gray) or ATR (purple) siRNA and sorted by FACS as in Figure 1G.

In all panels, data are presented as the mean of three independent experiments ± SD.

See also Figure S1.

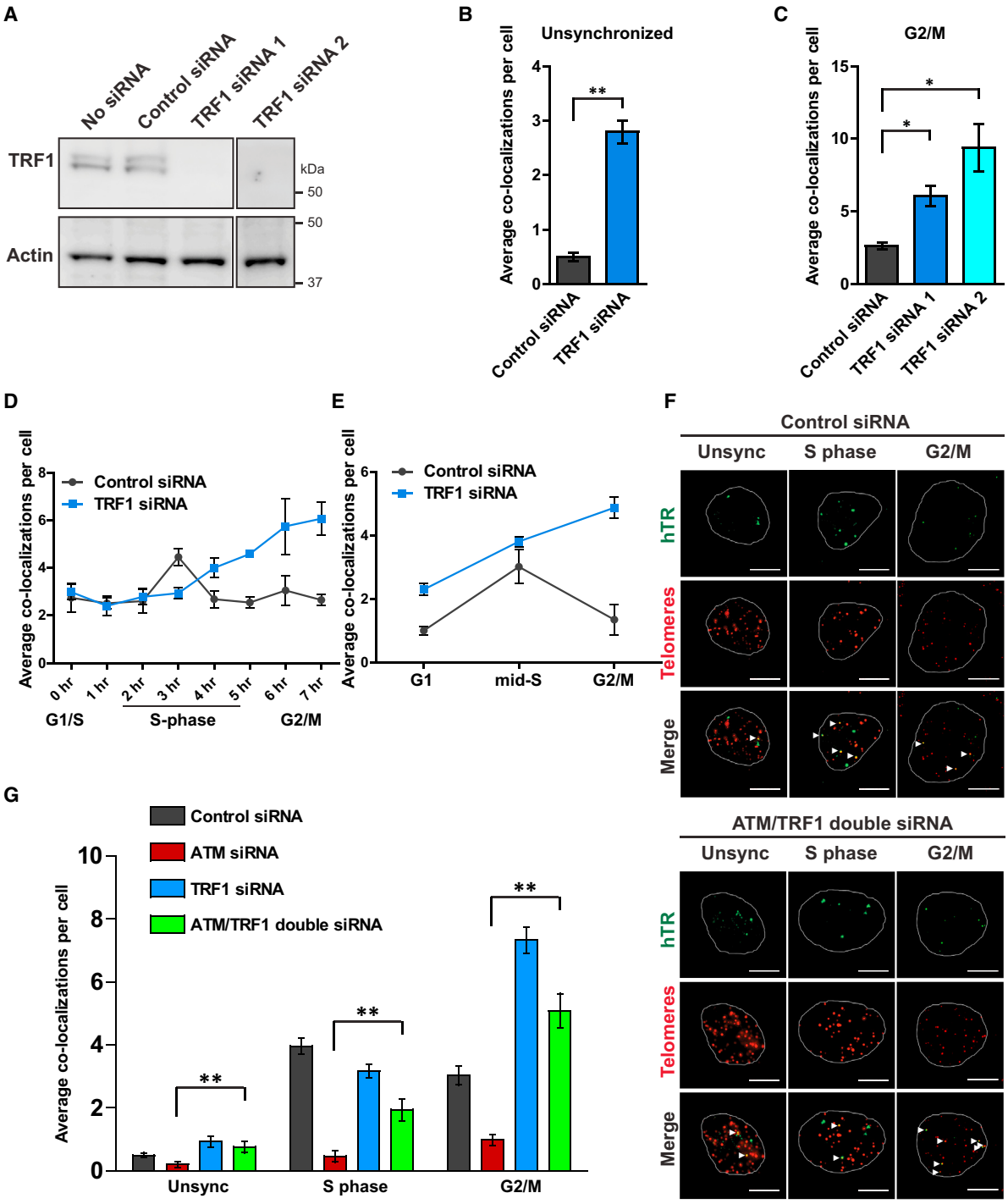

Figure 2. ATM Effect on Telomerase Recruitment Is Partially Mediated by TRF1

(A) Immunoblot of 293T cells treated with control or two different TRF1 siRNAs. All lanes are from the same immunoblot, which was cropped to remove intervening irrelevant lanes. Actin was probed as a control.

(B) Average recruitment of telomerase to telomeres in asynchronous 293T cells treated with control (gray) or TRF1 (blue) siRNA; **p = 0.0011.

(C) Average co-localization of telomerase with telomeres in 293T cells synchronized to G2/M of the cell cycle by release from a thymidine/aphidicolin block; cells were treated with control (gray) or two different TRF1 siRNAs (blue); *p < 0.05.

(D) Telomerase co-localization with telomeres in thymidine/aphidicolin synchronized 293T cells, treated with control (gray) or TRF1 (blue) siRNA. The values along the x axis represent the number of hours since release of cells from G1/S boundary. The control data are the same as those in Figure 1F, since these experiments were performed simultaneously.

(legend continued on next page)

~70%–80% with two independent siRNAs (Figures 2A, S2A, and S2B) and examined hTR-telomere colocalization. Knockdown of TRF1 resulted in large increases in telomerase recruitment in asynchronous cells or in cells synchronized to G2/M (Figures 2B, 2C, and S2C). Analysis of telomerase recruitment over the cell cycle revealed a deregulation of recruitment, particularly in G2/M phase, in both thymidine/aphidicolin synchronized and FACS-sorted 293T and HeLa cells (Figures 2D, 2E, and S2F–S2H). TRF1 knockdown also resulted in increased hTR/telomere co-localizations in G1 phase in FACS-sorted cells, demonstrating that TRF1 is involved in the signaling pathway that restricts telomerase presence at the telomere to S phase.

To confirm that ATM and TRF1 function in the same pathway, we performed a double knockdown of ATM and TRF1 (Figures S2D and S2E). If ATM involvement in telomerase recruitment is mediated by the phosphorylation and removal from the telomere of TRF1 (Wu et al., 2007), we predict that depletion of TRF1 will render telomerase insensitive to the absence of ATM. Simultaneous knockdown of ATM and TRF1 significantly elevated the levels of telomerase recruitment in S and G2/M phases compared to depletion of ATM alone ($p = 0.0018$ and $p = 0.0097$, respectively) (Figures 2F and 2G). A full recovery of recruitment was not observed in S phase cells; this may be partially due to residual TRF1 remaining after knockdown, but it also indicates that other TRF1-independent ATM substrates may be involved in telomerase recruitment (discussed further below).

Phosphorylation of TRF1 at Serine 367 Controls TRF1 and Telomerase Localization to Telomeres

We have demonstrated that phosphorylation of serine 367 of TRF1 results in localization of TRF1 to proteasome centers for degradation, resulting in telomere elongation (McKerlie et al., 2012). To demonstrate that such elongation events are due to changes in telomerase localization to telomeres, we transiently expressed in 293T cells similar levels of myc-tagged wild-type (WT) TRF1 or TRF1 containing mutations at S367 that either abolish (S367A) or mimic (S367D) phosphorylation at this residue (Figures 3A, S3A, and S3B). Exogenous TRF1 was expressed at levels 10- to 15-fold greater than endogenous TRF1 (Figure 3A); this level of overexpression was sufficient for replacement of endogenous TRF1 with myc-tagged exogenous TRF1 at ~25% of telomeres (Figures 3B–3E). S367D TRF1 demonstrated lower telomere association across all phases of the cell cycle than WT or S367A TRF1 (Figures 3B, 3D, and S3C), consistent with its inability to bind telomeric DNA in vitro (McKerlie et al., 2012). Endogenous TRF1 was not depleted in this experiment, since we expected S367D TRF1 to behave in a dominant-negative manner to sequester endogenous TRF1 from the telomere, as has been observed for other DNA-binding-defective TRF1 mutants (van Steensel and de Lange, 1997); we confirmed this using immunofluorescence with an antibody against TRF1 (Figures 3C and 3E). This observation coincided with an elevated level of telomerase recruitment in the presence of S367D TRF1 in G1 and G2/M phases (Figures 3B, 3F, and S3C). Deregulation of telomerase recruitment in G1 and G2/M phases upon both TRF1 knockdown and S367D TRF1 expression was confirmed in a HeLa cell line stably expressing a small hairpin RNA (shRNA) against TRF1, together with shRNA-resistant S367D TRF1 (McKerlie et al., 2012; Figure S3D).

Conversely, there was an ~50% decrease in telomerase recruitment at S phase in the presence of phosphodeficient S367A TRF1 compared to WT TRF1 in both 293T and HeLa cells (Figures 3F and S3D). These data suggest that phosphorylation of TRF1 at serine 367 results in dissociation of a portion of TRF1 from telomeres during S phase and that this is necessary for full telomerase recruitment. This is supported by the slight increase in levels of endogenous TRF1 at telomeres in G2/M relative to S phase (Figures 3C and 3E). However, depletion of TRF1 levels at the telomere using siRNA, shRNA, or expression of the dominant-negative S367D TRF1 did not lead to substantially increased telomerase at the telomere during S phase (Figures 2D–2G, S2H, 3E, 3F, and S3D), suggesting that removal of TRF1 is necessary, but not sufficient, for full telomerase recruitment in S phase. Together, our data show that the major function of TRF1 is in the displacement of telomerase from the telomere *outside* S phase, for which removal of the phosphate group at S367 appears to be necessary.

Stalled Replication Forks Trigger Telomerase Recruitment

The mechanism of telomerase regulation at the telomere by TRF1 may involve the known role of TRF1 in facilitating replication of telomeric DNA (Sfeir et al., 2009). Repetitive telomere repeats represent challenging templates for the canonical DNA replication machinery, often resulting in stalled replication forks and recruitment of the single-stranded DNA-binding protein RPA and activation of ATR (Ohki and Ishikawa, 2004; Sfeir et al., 2009; Fouché et al., 2006; Ivessa et al., 2002); in mammalian cells, this phenotype is exacerbated by depletion of TRF1 (Sfeir et al., 2009; Martínez et al., 2009). Our observation that treatment of cells with aphidicolin and thymidine results in an apparent increase in numbers of hTR-telomere foci (Figures 1F and 1G) suggests that DNA damage directly regulates telomerase recruitment. To directly examine whether this effect can be attributed to stalled replication forks, we subjected

(E) Telomerase co-localization with telomeres in 293T cells, treated with control (gray) or TRF1 (blue) siRNA; cells were stained with the DNA dye VyBrant DyeCycle Violet and isolated into the cell-cycle phases with FACS. The control data are the same as those in Figure 1G, since these experiments were performed simultaneously.

(F) FISH for hTR (green) and telomeres (red) in 293T cells treated with control or combined ATM and TRF1 siRNAs. Cells were either asynchronous or synchronized with thymidine and aphidicolin and harvested 3–4 hr (S phase) or 7 hr (G2/M) after release from the G1/S boundary. Co-localizations are indicated by the white arrows in the merge row. Scale bar, 10 μm.

(G) Quantitation of (F); average telomerase-telomere co-localizations after control (gray), ATM only (red), TRF1 only (blue), and ATM/TRF1 (green) siRNAs, in asynchronous, S phase, or G2/M phase cell populations; $n = 4$; $^{**}p < 0.01$.

Data are presented as the mean of three independent experiments except where indicated otherwise, ± SD.

See also Figure S2.

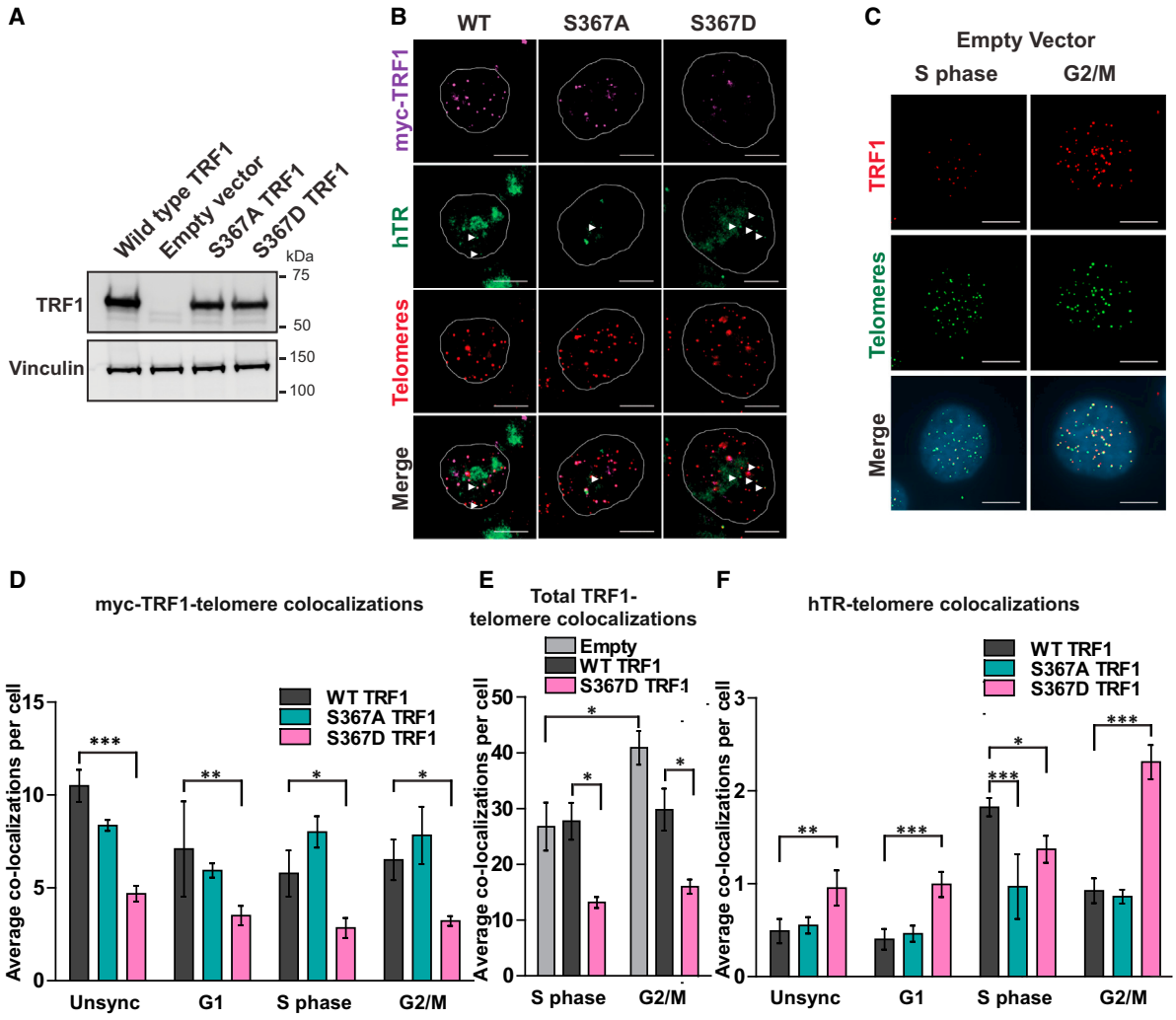

Figure 3. Phosphorylation of TRF1 at Serine 367 Regulates TRF1 and Telomerase Localization to Telomeres

(A) Immunoblot of overexpressed myc-tagged WT TRF1, empty vector, myc-S367A TRF1, or myc-S367D TRF1, probed with an anti-TRF1 antibody and with vinculin probed as a control.

(B) Immunofluorescence with an anti-myc antibody (purple) and hTR/telomere FISH (green and red respectively) in asynchronous 293T cells overexpressing myc-tagged WT, S367A, or S367D TRF1. Co-localizations between hTR and telomeres are indicated by white arrows. Scale bar, 10 μm.

(C) Immunofluorescence with an anti-TRF1 antibody (red) and telomere FISH (green) in 293T cells transfected with empty vector and sorted into S or G2/M phase based on DNA content. Scale bar, 10 μm.

(D) Quantitation of average co-localization of overexpressed myc-tagged TRF1 with telomeres across cell-cycle stages in FACS sorted 293T cells; *$p < 0.05$, **$p < 0.01$, ***$p < 0.005$.

(E) Quantitation of total TRF1 at telomeres in S and G2/M phase sorted 293T cells overexpressing myc-tagged WT TRF1, empty vector, or myc-S367D TRF1; *$p < 0.05$.

(F) Quantitation of average co-localization of hTR and telomeres across cell-cycle stages in FACS-sorted 293T cells overexpressing myc-tagged WT TRF1, myc-S367A TRF1, or myc-S367D TRF1; *$p < 0.05$, **$p < 0.01$, ***$p < 0.005$.

In all panels, data are presented as the mean of three independent experiments ± SD.

See also Figure S3.

asynchronous 293T cells to a much shorter period of aphidicolin treatment. Telomerase recruitment increased ~2-fold after 30-min treatment with 0.5 μg/ml aphidicolin compared to controls, despite no significant change in cell-cycle profile, and this increase was dependent upon ATR (Figures 4A, 4B, and S4). Phosphorylation of the ATR target protein Chk1 demonstrated that a 30-min treatment with aphidicolin was sufficient to cause replication problems and activate the ATR pathway (Figure 4C). To ensure that this aphidicolin treatment did not result in damage signaling from DNA double-strand breaks (DSBs) arising from collapsed replication forks, we examined activation of the ATM-Chk2 DSB response pathway (Figure 4C).

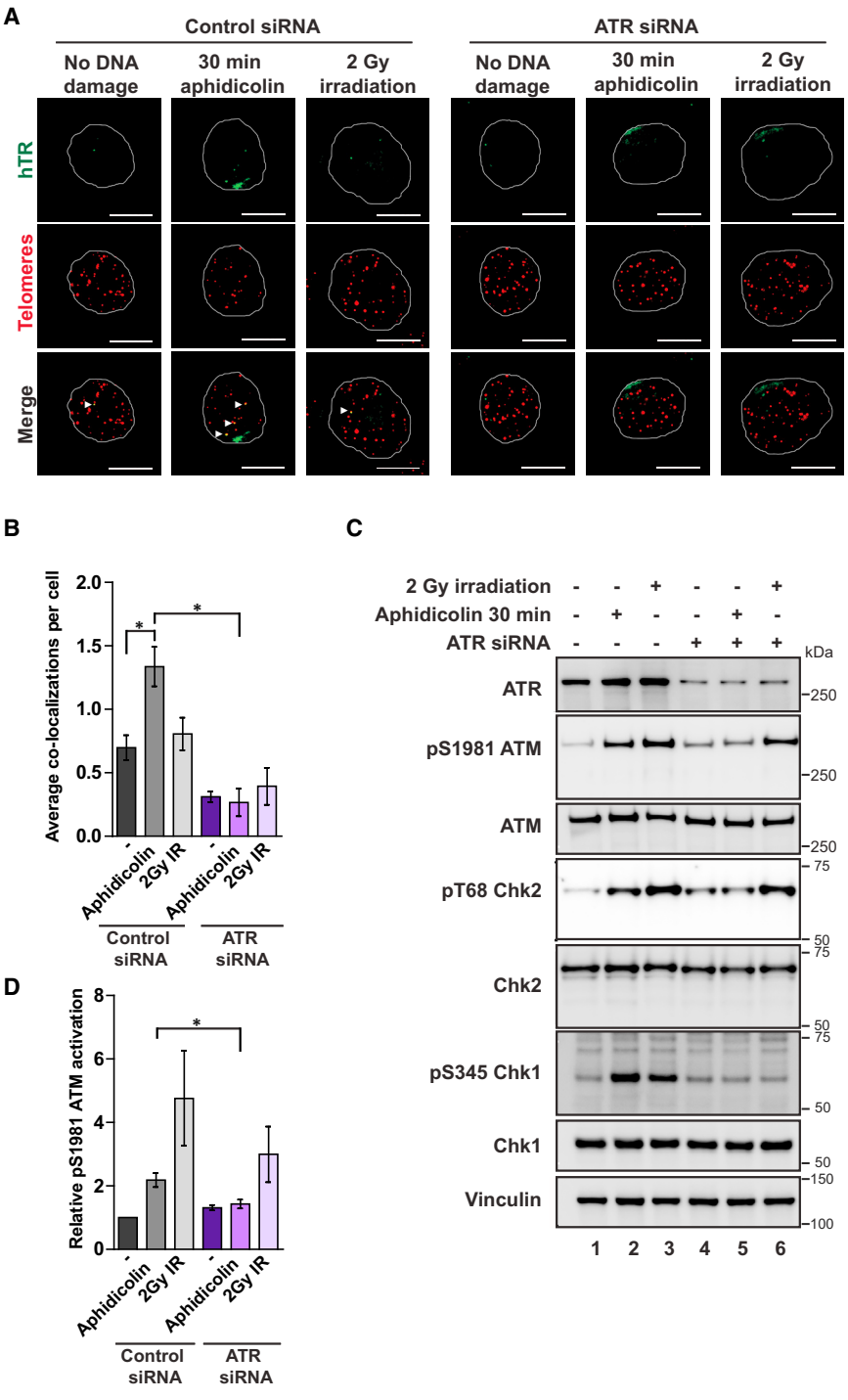

Figure 4. Stalled Replication Forks Trigger Telomerase Recruitment

(A) FISH for hTR (green) and telomeres (red) in asynchronous 293T cells treated with control (three left panels) or ATR (three right panels) siRNA. DNA damage was induced by either 30 min of aphidicolin treatment to induce stalled replication forks or 2 Gy gamma irradiation to induce double-strand breaks. Co-localizations between hTR and telomeres are indicated by the white arrows. Scale bar, 10 μm.

(B) Quantitation of telomerase localization to telomeres in cells from Figure 4A; *p < 0.05.

(C) Immunoblot of cells treated as in Figure 4A, probed for ATR, pS1981 ATM, ATM, pT68 Chk2, Chk2, pS345 Chk1, Chk1, and vinculin as a control.

(D) Quantitation of ATM activation (pS1981 ATM levels) from blot in Figure 4C; *p = 0.028.

In all panels, data are presented as the mean of three independent experiments ± SD.

See also Figure S4.

Aphidicolin treatment caused a moderate activation of ATM and Chk2 phosphorylation (Figure 4C, lane 2, and Figure 4D), but this was abolished by knockdown of ATR (Figure 4C, lane 5, and Figure 4D), indicating that it results from the direct activation of ATM by ATR that is known to occur upon replication fork stalling (Stiff et al., 2006) rather than from DSB formation. In addition, induction of DSBs by gamma irradiation triggered robust ATR-independent ATM activation (Figure 4C, lanes 3 and 6) that did not result in increased telomerase recruitment to telomeres (Figures 4A and 4B). Together, our data demonstrate that an increase in stalled replication forks and the resulting ATR signaling result in an increase in telomerase presence at the telomere. This is consistent with the telomere lengthening previously observed in telomerase-positive human cells after long-term treatment with aphidicolin (Sfeir et al., 2009).

Telomere Elongation Triggered by POT1 Mutation Is Dependent on ATM

As a TRF1-independent mechanism of exposing single-stranded DNA at telomeres, we infected HeLa204 cells (Takai et al., 2010) with a retrovirus encoding the human POT1 construct myc-POTΔOB (Loayza and De Lange, 2003). Myc-POT1ΔOB contains a truncation of one of the two POT1 OB folds, allowing POT1 to localize to telomeres but abolishing its ability to bind single-stranded telomeric DNA and abrogating POT1-mediated telomere-length regulation (Loayza and De Lange, 2003; Zhong et al., 2012). As expected, myc-POTΔOB caused dramatic telomere-length elongation over 35–37 population doublings (PDs) (Figure 5A). Simultaneous expression of three independent shRNAs against ATM (Figure 5B) completely abrogated telomere lengthening (Figure 5A), demonstrating that telomerase-mediated telomere lengthening in this context is dependent on ATM.

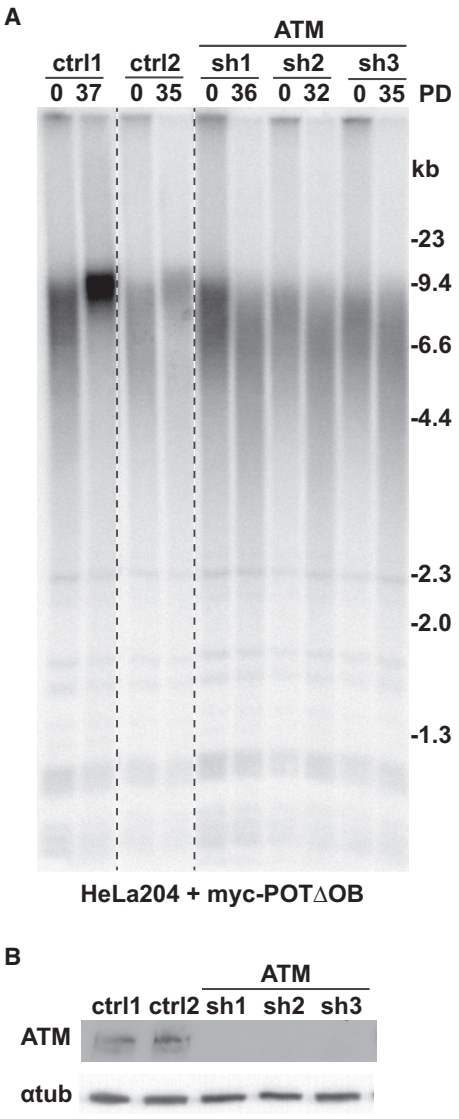

Figure 5. Telomere Elongation Triggered by POT1 Mutation Is Dependent on ATM

(A) Terminal restriction fragment (TRF) assay to determine telomere length. HeLa204 cells were infected with retrovirus encoding luciferase shRNA (ctrl1), no shRNA (ctrl 2), or three different ATM shRNAs, together with myc-POT1ΔOB overexpression, and cultured for 32–37 population doublings (PDs). All lanes are from the same blot, which was cropped to remove intervening irrelevant lanes.

(B) Immunoblot to determine ATM knockdown following shRNA treatment of cells from (A), with α-tubulin as a control.

ATM and ATR Also Affect Telomerase Complex Assembly

The inability of TRF1 depletion to completely rescue telomerase recruitment after ATM silencing (Figure 2G) implies that ATM can affect other TRF1-independent pathways of telomerase regulation. We therefore investigated the levels of cellular telomerase components and their assembly capabilities. Measurement of total cellular hTR levels with a dot blot using an hTR-specific probe revealed a slight inhibitory effect of TRF1 siRNA on hTR abundance (Figures 6A, 6B, S5A, and S5B). The amount of hTR recovered after immunoprecipitation with an antibody against hTERT (Figures 6A and 6C) reflected the levels of hTR in crude lysates, indicating that TRF1 depletion did not impact assembly of hTERT and hTR into an active complex. Conversely, treatment with ATM siRNA did not affect cellular hTR abundance (Figures 6A and 6B), but it reduced telomerase complex assembly by ~50% across all phases of the cell cycle (Figures 6A and 6C). Double ATM/TRF1 knockdown also resulted in a similar assembly defect (Figures 6D, S5C, and S5D), indicating that TRF1 is unlikely to be the ATM target responsible for this effect. Telomerase activity, measured by a direct non-PCR assay (Cohen and Reddel, 2008) and normalized against the amount of hTR recovered in hTERT immunoprecipitates, revealed no significant changes in the specific activity of telomerase after depletion of either ATM or TRF1 (Figures 6E, 6F, S5E, and S5G).

We also examined the effect of ATR silencing on levels of cellular telomerase RNA and telomerase assembly. Treatment with two different ATR siRNAs (Figure S5H) reduced telomerase complex assembly by up to ~50% in unsynchronized and G1 phase cells (Figures 6G and 6H) without affecting total hTR levels or specific activity of telomerase (Figures 6I and S5I–S5K).

DISCUSSION

In this study, we have demonstrated that ATM and ATR are both necessary for full telomerase recruitment to telomeres in human cell lines. This conclusion is supported by an independent study using complementary approaches in which ATM was demonstrated to be necessary for telomerase-mediated telomere addition in both human and mouse cells (Lee et al., 2015). This provides an explanation, at least in part, for the long-standing observation of short telomeres in the ATM-deficient cells of ataxia telangiectasia (AT) patients (Metcalfe et al., 1996; Smilenov et al., 1997) and the telomere shortening observed upon inhibition of ATM in telomerase-positive immortal human cell lines (Wu et al., 2007). Consistently, while AT patient cells can become immortalized by activation of telomerase, most of these cell lines harbor very short telomeres (Sprung et al., 1997).

Our data show that TRF1 is involved in the signaling pathway restricting telomerase access to the telomere to S phase; loss of TRF1 results in an increase in telomerase at the telomere in both G1 and G2/M phases. Evidence from this and previous studies suggests that phosphorylation of TRF1 at serine 367 results in partial TRF1 dissociation from telomeres and its degradation; removal of this phosphate is necessary for correct cell-cycle control of telomerase presence at the telomere. Constitutive expression of a phosphomimetic of S367 TRF1 also leads to inappropriate retention of telomerase at the telomere outside S phase, leading to a telomere-length increase (Wu et al., 2007; McKerlie et al., 2012; this study; Figure 3). The mechanism for this regulatory function of TRF1 may include its known role in facilitating telomere replication; TRF1 dissociation from telomeres induces replication fork stalling that activates ATR (Sfeir et al., 2009), and we provide evidence that replication fork stalling leads to an ATR-dependent increase in telomerase recruitment (Figure 4). The control of telomere replication and

telomerase presence at the telomere by human TRF1 (Figure 7A) appears analogous to the situation in *Schizosaccharomyces pombe,* in which deletion of the double-stranded telomeric-binding protein Taz1 results in stalled telomeric replication forks (Miller et al., 2006) and leads to deregulation of the cell-cycle control of telomerase at the telomere (Dehé et al., 2012; Chang et al., 2013). It is possible that in the absence of TRF1, aberrant products of stalled replication forks may persist into the subsequent G2/M and G1 phases, forming substrates for telomerase, as has been postulated in the case of Taz1 in *S. pombe* (Dehé et al., 2012). It has been proposed that it is the tendency of the replication machinery to stall in repetitive DNA that forms the signal for telomerase recruitment specifically in S phase (Rog and Cooper, 2008; Verdun and Karlseder, 2006; Wu et al., 2007; Stern and Bryan, 2008; Dehé et al., 2012; Chang et al., 2013). In this report, we provide direct evidence for this concept.

The downstream targets of ATR involved in mediating human telomerase recruitment have not yet been identified. Under stalled fork conditions, activated ATR is able to phosphorylate and activate ATM (Stiff et al., 2006, and Figures 4C and 4D); whether this phosphorylation of ATM participates in a positive feedback loop in removing TRF1 to accelerate ATR-mediated telomere length regulation remains to be investigated.

We also provide evidence that exposing telomeric single-stranded DNA in a different way, by overexpression of POT1 lacking its DNA-binding domain (Loayza and De Lange, 2003), provides a signal for rapid telomere lengthening that is also ATM dependent (Figure 5). Overexpression of POTΔOB does not perturb binding of TRF1 to the telomere (Loayza and De Lange, 2003); the ATM-dependence of telomere lengthening in this context reinforces the notion that in addition to mediating telomerase recruitment through a TRF1-dependent pathway, there must be other TRF1-independent mechanisms by which ATM mediates telomerase localization at telomeres. This is consistent with the observation that lack of TRF1 does not completely rescue the telomerase recruitment defect caused by ATM depletion (Figure 2G).

We demonstrated that one TRF1-independent function of ATM is its impact upon the ability of hTR and hTERT to assemble into a functional enzyme complex (Figure 6), which is a prerequisite for localization of hTR to telomeres (Tomlinson et al., 2008). ATR also plays a role in assembly of human telomerase; we do not know if the substrates of these two kinases in this process are the same. This role is reflected in a substantial decrease in the amount of hTR recovered after hTERT immunoprecipitation and in the total immunoprecipitated telomerase activity following ATM and ATR knockdown. The specific activity of telomerase remains unchanged, demonstrating that both ATM and ATR have no effect on telomerase catalytic activity, consistent with results in yeast (Chan et al., 2001). No consensus PIKK phosphorylation motifs exist in the RNA-binding domain of hTERT, implying either that ATM or ATR can mediate telomerase assembly by targeting regions not in the RNA-binding domain or that they can regulate telomerase assembly by phosphorylating unknown substrates (Figure 7B).

Our data support a model incorporating multiple roles for ATM and ATR in the presence of human telomerase at telomeres (Figure 7). One pathway involving both ATM and ATR is mediated by phosphorylation of TRF1 and its removal from the telomere, leading to replication fork stalling in telomeric DNA, which acts as a trigger for telomerase recruitment. A second pathway involves the role of ATM and ATR in facilitating telomerase assembly; additional phosphorylation targets of ATM, ATR, and other PIKKs in the telomerase recruitment process may remain to be identified. These data reveal that although it is important for telomeres to *repress* DNA damage signaling in order to avoid deleterious fusions, telomeres have also evolved the ability to carefully *exploit* aspects of DNA damage signaling pathways to regulate telomerase presence at the telomere. Increased understanding of regulation of telomerase assembly and access to the telomere may provide valuable insight in the process of developing highly specific cancer therapeutics.

EXPERIMENTAL PROCEDURES

Plasmids

A TRF1 expression plasmid containing myc-tagged TRF1 was constructed by subcloning the TRF1 open reading frame from pCMV-GFP.hTRF1 plasmid into a pcDNA3.1/myc-HisB plasmid by In-Fusion cloning (Clontech Laboratories) according to the manufacturer's protocol. The mutation of serine 367 of TRF1 into alanine or aspartic acid was achieved using the Stratagene QuikChange II XL Site-Directed Mutagenesis kit. POT1 lacking the OB fold domain (POT1ΔOB) was expressed from the pLPC retroviral vector as described (Loayza and De Lange, 2003), followed by infection with retrovirus vectors encoding shRNAs against ATM.

Cell Culture and Transfections

HEK293T cells (from Dr. T. Adams, CSIRO), HeLa cells (American Type Culture Collection), HeLa204 cells (Takai et al., 2010), or HeLa cells stably overexpressing TRF1 (McKerlie et al., 2012) were cultured in DMEM supplemented with 10% fetal bovine serum (FBS) in a humidified 37°C incubator with 5% CO_2. Cells were transfected with 90 pmol siRNA and 5.5 μl Lipofectamine RNAiMAX (Life Technologies) in 310 μl Opti-MEM (Life Technologies). siRNA sequences and catalog numbers are provided in Table S1. Cells overexpressing myc-TRF1 were transfected with 2.5 μg WT TRF1 or 1.0 μg S367A/D TRF1 expression plasmid to ensure even protein expression levels, in DMEM for 34 hr. HEK293T cells were then synchronized at G1/S phase by adding 2 mM thymidine (Sigma-Aldrich) for 15 hr, releasing for 9 hr, and adding 0.5 μg/ml aphidicolin (Sigma-Aldrich) for 16 hr. Cells were harvested 3 hr after release and confirmed to be in mid-S phase by analysis of DNA content by flow cytometry on a FACSDiva (Becton Dickinson). HeLa cells grown in DMEM media (+ 10% FBS) were synchronized with medium containing 2 mM thymidine (Sigma-Aldrich) for 18 hr, released into thymidine-free DMEM (+ 10% FBS) for 9 hr and blocked with a second round of 2 mM thymidine for 15 hr. For kinase inhibitor treatment, 1.5 μM KU-55933 (Merck Millipore), 500 mM VE-822 (Selleckchem), or DMSO was added to cells released from synchronization for 3 hr before harvesting in mid-S phase.

For cell sorting, cells were harvested and resuspended in Hank's balanced salt solution (Life Technologies) at a concentration of 1×10^6 cells/ml. The cells were stained with VyBrant DyeCycle Violet (Life Technologies) at a concentration of 1 μl per 1×10^6 cells at 37°C for 30 min before cell sorting using a BD FACSAriaIII Cell Sorter (BD Biosciences). Confirmation of cell-cycle phases was performed using the FACSDiva (Becton Dickinson).

Gamma Irradiation

Gamma irradiation was performed using the Gammacell 1000 Elite irradiator (Best Theratronics) with a ^{137}Caesium source. The irradiated cells were returned to incubate at 37°C for an hour before harvesting for downstream analysis.

FISH of hTR and Telomeric DNA, and Immunofluorescence

Simultaneous FISH against hTR and telomeric DNA, with or without immunofluorescence for TRF1, was performed as previously described (Stern et al.,

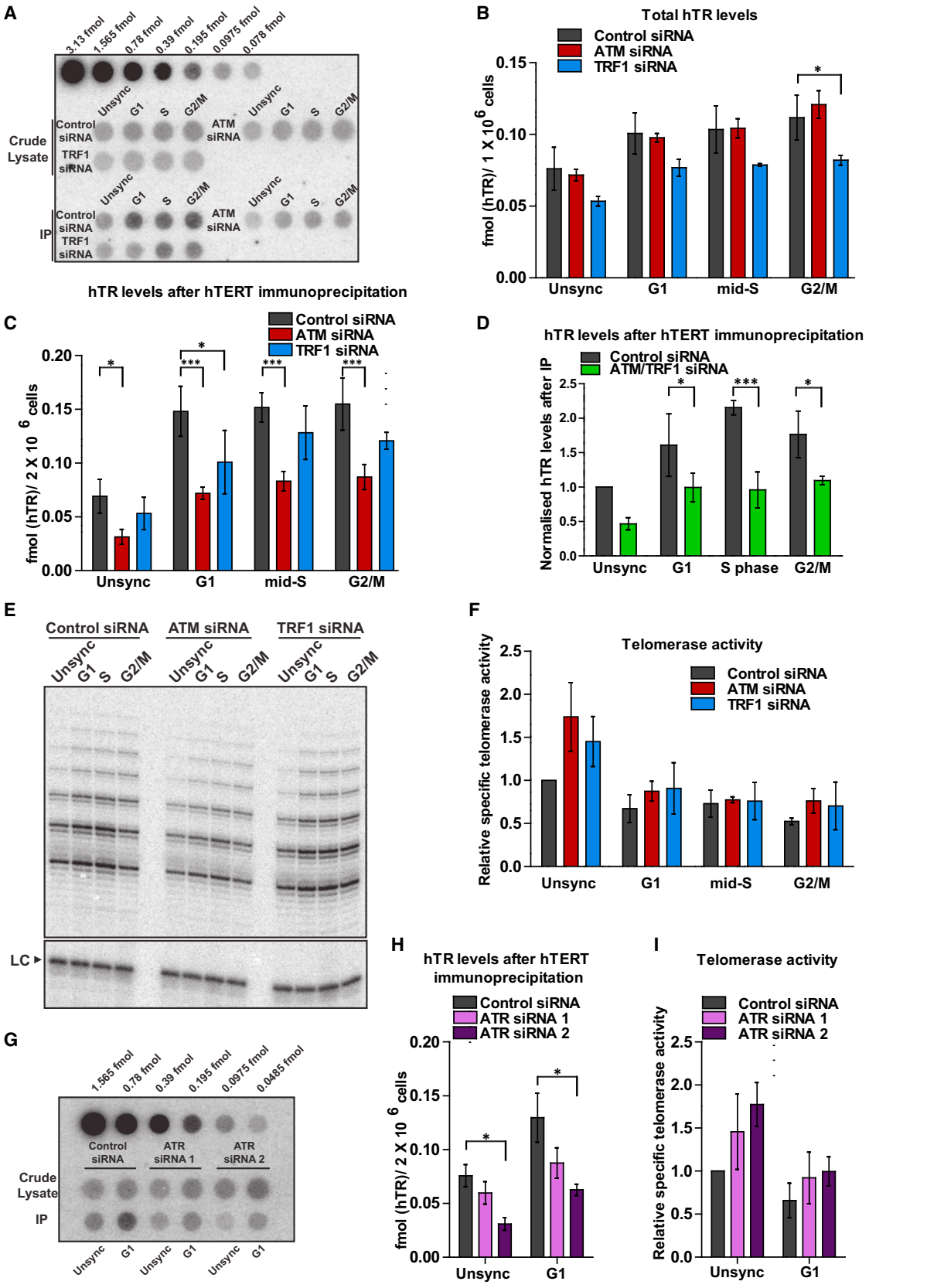

(legend on next page)

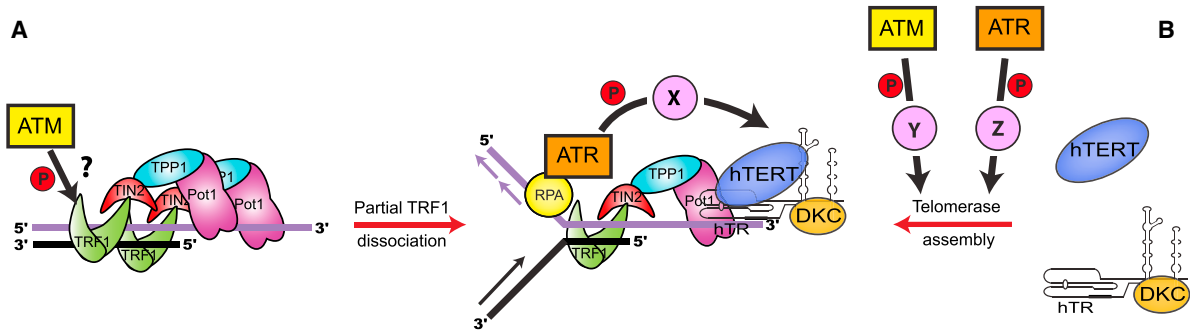

Figure 7. Model for ATM and ATR Involvement in Human Telomerase Recruitment to Telomeres

(A) During S phase, ATM and/or other PIKKs phosphorylates TRF1 at S367, which leads to partial dissociation of TRF1 from telomeres (McKerlie et al., 2012; Wu et al., 2007). Depletion of TRF1, together with its protein partners Tin2, TPP1, and Pot1, causes telomeric replication forks to stall, leading to recruitment of RPA and ATR (Sfeir et al., 2009; Martínez et al., 2009; Zimmermann et al., 2014). ATR phosphorylates an unknown substrate to mediate telomerase recruitment. Replication fork stalling caused by aphidicolin treatment also leads to telomerase recruitment (this study) and telomere elongation (Sfeir et al., 2009).

(B) An independent role of ATM and ATR involves stimulation of telomerase assembly, which is a prerequisite for telomerase localization to telomeres. This model does not preclude involvement of other unidentified substrates of ATM, ATR, and other PIKKs.

2012), with the exception that cells were fixed in 2% paraformaldehyde. Antibodies used for immunofluorescence were Myc-tag antibody (Cell Signaling, cat. no 2276; diluted 1:1,000) and polyclonal rabbit anti-TRF1 antibody (#370, de Lange lab; diluted 1:2,000). Staining was visualized on a Zeiss Axio Imager M1 microscope, with a Plan-Apochromat 63× oil objective (numerical aperture, 1.4), and an AxioCam MR digital camera (Carl Zeiss). Exposure times between treatments were consistent. For presentation purposes, pixel intensity histograms were adjusted in ZEN (Carl Zeiss), equally across all figure panels, and images were cropped in Adobe Photoshop. Colocalizing hTR and telomere foci were manually counted in >100 cells per treatment, and data were analyzed by Student's t test for pairwise comparison.

Automated Quantification of 3D Co-localizations between TRF1 and Telomeres

Immunofluorescence with anti-TRF1 antibody (Figure 3C) had sufficiently low background that quantitation of colocalizing foci was able to be automated using Metafer4 software (Metasystems) on a Zeiss Axioplan 2 microscope (Germany), with a 63× NA (1.4 Plan-Apochromat) oil objective, and appropriate filter cubes. DAPI stained nuclei were identified and background subtraction, image sharpening and TopHat transformation applied to the TRF1 immunofluorescence and telomere FISH channels. TRF1 immunofluorescence and telomere FISH foci were defined as foci of >0.1 μm^2, >25% intensity over background, separated by a minimum distance of 0.5 μm. Co-localizations were events where the center of a TRF1 and a telomere FISH focus were $\leq$0.3 μm apart in three dimensions. Colocalizing TRF1 and telomere foci were counted in 200–300 cells per treatment, and data were analyzed by Student's t test for pairwise comparison.

Cell Lysis and Western Blot

The procedure for cell lysis and western blot was performed as previously described (Guo et al., 2014), with the exception that the large proteins ATR and ATM were electrophoresed on 3%–8% gradient Tris-Acetate gels (Life Technologies) at 150 V for 90 min. The following antibodies were used: ATM (Abcam rabbit polyclonal, diluted 1:2,000, cat. no AB32420), ATR (Cell Signaling rabbit polyclonal, diluted 1:1,000, cat. no 2790), anti-pS1981 ATM (Abcam rabbit polyclonal, diluted 1:1,000, cat. no AB81292), pT68 Chk2 (Cell Signaling rabbit polyclonal, diluted 1:1,000, cat. no 2661), Chk2 (Merck-Millipore mouse monoclonal, diluted 1:1,000, cat. no 05-649), pS345 Chk1 (Cell Signaling rabbit polyclonal, diluted 1:1,000, cat. no 23485), Chk1 (Cell Signaling mouse monoclonal, diluted 1:1,000, cat. no 23605), TRF1 (rabbit polyclonal, #370, de Lange lab, diluted 1:2,000), vinculin (Sigma-Aldrich mouse monoclonal, diluted 1:10,000, cat. no V9131), and actin (Sigma-Aldrich rabbit polyclonal, diluted 1:10,000, cat. no A2103).

qRT-PCR

RNA extraction was performed using the RNeasy Mini Kit (QIAGEN) according to manufacturer's protocol and RNA quantitated with a Nanodrop spectrophotometer (ThermoFisher ND-1000). RNA (1 μg) was digested with 1 U of DNase

Figure 6. ATM Affects Telomerase Assembly

(A) Dot blot for hTR in 293T cells treated with control, ATM, or TRF1 siRNA and synchronized with thymidine/aphidicolin. Crude cell lysates (top panel) contain total levels of cellular hTR, while hTERT immunoprecipitated samples (IP) contain only hTR that has assembled with hTERT. Top row: in-vitro-transcribed hTR standard.

(B) Quantitation of total hTR levels following control (gray), ATM (red), or TRF1 (blue) siRNA treatments (fmol of hTR in 1 × 10^6 cells) from (A); *p = 0.032.

(C) Quantitation of hTR assembled with hTERT (fmol of hTR in 2 × 10^6 cells) from (A), following control (gray), ATM (red), or TRF1 (blue) siRNA treatments; *p < 0.05, ***p < 0.005.

(D) Quantitation of hTR assembled with hTERT after treatment with combined ATM and TRF1 siRNAs (green); *p < 0.05, ***p < 0.005.

(E) Direct telomerase activity assay of immunoprecipitated telomerase from cells treated with control, ATM, and TRF1 siRNA, synchronized to the indicated cell-cycle stages. LC represents an 18-nt loading control.

(F) Telomerase specific activity, derived from total telomerase activity (Figure 6E) normalized to levels of hTR after hTERT immunoprecipitation (Figure 6C).

(G) Dot blot for hTR in 293T cells treated with control or two different ATR siRNAs and synchronized with thymidine/aphidicolin. The combination of ATR siRNA and thymidine/aphidicolin treatment perturbs progression of the cells through S phase, so this experiment could only be performed on unsynchronized or G1 cells. Crude cell lysates (top panel) contain total levels of cellular hTR, while hTERT immunoprecipitated samples (IP) contain only hTR that has assembled with hTERT. Top row: in-vitro-transcribed hTR standard.

(H) Quantitation of hTR assembled with hTERT after treatment with two different ATR siRNAs (purple); *p < 0.05.

(I) Telomerase specific activity, derived from total telomerase activity (Figure S5K) normalized to levels of hTR after hTERT immunoprecipitation (Figure 6H).

In all panels, data are presented as the mean of three independent experiments ± SD.

See also Figure S5.

(Amp grade; Sigma-Aldrich) at room temperature for 15 min, before the addition of EDTA to 2.5 mM and heat inactivation at 65°C. cDNA synthesis was performed using the Superscript III First-Strand Synthesis System for RT-PCR (Life Technologies) according to the manufacturer's protocol. qPCR was performed in triplicate on each cDNA with corresponding GAPDH controls, using the Roche real-time PCR LightCycler 96 system with 45 cycles of 95°C for 15 s and 60°C for 60 s, in Applied Biosystems SYBR green mix, with 0.5 μM forward and reverse primers (TRF1 forward: 5′-CGAGCTAGAAAAAGACAGGC-3′, TRF1 reverse: 5′-AGTTTTAGTTTCTTCATGGT-3′, GAPDH forward: 5′-ACCCA CTCCTCCACCTTTG-3′, GAPDH reverse: 5′-CTCTTGTGCTCTTGCTGGG-3′). Analysis was carried out using the ΔΔCt method with the Roche LightCycler 96 system software.

hTR Dot Blot

Harvested cells were lysed with telomerase buffer (20 mM HEPES-KOH [pH 7.9], 300 mM KCl, 2 mM $MgCl_2$, 10% v/v glycerol, 0.1% v/v Triton X-100, 5 mM DTT, 1 mM PMSF) at a concentration of 10^5 cells/μl, rotating at 4°C for 1 hr before centrifugation at 16,200 × *g* at 4°C for 20 min. 10 μl of the lysate was applied to a GE Healthcare Life Sciences Amersham Hybond-XL membrane and probed with a ^{32}P-labeled oligonucleotide complementary to hTR as described previously (Jurczyluk et al., 2011).

Telomerase Purification and Activity Assay

Immunopurification of telomerase was performed as described elsewhere (Cohen and Reddel, 2008), using a polyclonal anti-hTERT antibody and elution with a competing peptide (both available from Abbexa). Activity of the eluted telomerase was measured in a 20 μl solution phase extension reaction containing 20 mM HEPES-KOH (pH 7.9), 2 mM $MgCl_2$, 5 mM DTT, 1 mM spermidine, 0.1% Triton X-100, 0.5 mM dTTP, 0.5 mM dATP, 5 μM α-^{32}P-dGTP (198 Ci/mmol), and 1 μM DNA primer Bio-L-18GGG (5′-biotin-CTAGACC TGTCATCA$(TTAGGG)_3$-3′) for 60 min at 37°C. The reaction was terminated with EDTA and products isolated on Dynabead M280 streptavidin beads (Life Technologies), together with a 12-nt biotinylated control DNA, as described previously (Tomlinson et al., 2015). Products were separated on a 10% acrylamide/7 M urea sequencing gel as described previously (Tomlinson et al., 2015).

Telomere Restriction Fragment Southern Blot

Telomere length was measured by *Hin*fI/*Rsa*I digestion of genomic DNA, separation by agarose gel electrophoresis, transfer to nylon membrane, and probing with a ^{32}P-labeled telomeric probe, using standard techniques (de Lange, 1992).

The hTERT antibody CMRI 276-294 and antigenic release peptide are available to researchers from Abbexa, under exclusive license from the authors' institution, Children's Medical Research Institute.

SUPPLEMENTAL INFORMATION

Supplemental Information includes five figures and one table and can be found with this article online at http://dx.doi.org/10.1016/j.celrep.2015.10.041.

AUTHOR CONTRIBUTIONS

J.L.S., A.S.T., and T.M.B. designed the project and conceived hypotheses; A.S.T. performed the majority of the experiments, with other experiments contributed by M.K. and J.L.S.; A.S. and T.d.L. contributed experiments related to Pot1ΔOB; all authors analyzed data and interpreted experimental results; and A.S.T. and T.M.B. wrote the manuscript with input from all authors.

ACKNOWLEDGMENTS

Cell sorting was performed in the Flow Cytometry Core Facility that is supported by Westmead Research Hub, Cancer Institute New South Wales (CINSW) and National Health and Medical Research Council (NHMRC). Microscopy was performed in the ACRF Telomere Analysis Centre, supported by Australian Cancer Research Foundation and the Ian Potter Foundation, and with the assistance of Scott Page. Phosphoimaging analysis was performed on a Typhoon Biomolecular Imager purchased with support from the Ramaciotti Foundation. We thank Sonja Frölich and Anthony Cesare for development of the algorithm used for automated foci counting. We are grateful to Anthony Cesare, Scott Cohen, and Christopher Tomlinson (Children's Medical Research Institute) for helpful discussions and providing protocols. We thank Angus Ho in the X.-D.Z. laboratory for the generation of TRF1-depleted HeLa cells complemented with WT and mutant TRF1 alleles. Work in the Bryan laboratory was supported by project grants awarded by Cancer Council NSW (RG10/02 and RG12/02) and NHMRC (571073). Work in the Zhu laboratory was supported by the Canadian Institutes of Health Research (MOP-86620). The work on telomere length regulation was supported by an RO1 from the NIH (to T.d.L.). A.S.T. was supported by a Kids Cancer Alliance PhD Scholarship, M.K. by an Australian Awards Scholarship, and T.M.B. by a Career Development Fellowship from CINSW (11/CDF/3-05). J.L.S. was supported by an NHMRC Biomedical Research scholarship, the CINSW Research Scholar Award, and the Judith Hyam Memorial Trust.

Received: June 23, 2015
Revised: September 14, 2015
Accepted: October 16, 2015
Published: November 12, 2015

REFERENCES

Abreu, E., Aritonovska, E., Reichenbach, P., Cristofari, G., Culp, B., Terns, R.M., Lingner, J., and Terns, M.P. (2010). TIN2-tethered TPP1 recruits human telomerase to telomeres *in vivo*. Mol. Cell. Biol. *30*, 2971–2982.

Ancelin, K., Brunori, M., Bauwens, S., Koering, C.E., Brun, C., Ricoul, M., Pommier, J.P., Sabatier, L., and Gilson, E. (2002). Targeting assay to study the cis functions of human telomeric proteins: evidence for inhibition of telomerase by TRF1 and for activation of telomere degradation by TRF2. Mol. Cell. Biol. *22*, 3474–3487.

Armbruster, B.N., Linardic, C.M., Veldman, T., Bansal, N.P., Downie, D.L., and Counter, C.M. (2004). Rescue of an hTERT mutant defective in telomere elongation by fusion with hPot1. Mol. Cell. Biol. *24*, 3552–3561.

Arnerić, M., and Lingner, J. (2007). Tel1 kinase and subtelomere-bound Tbf1 mediate preferential elongation of short telomeres by telomerase in yeast. EMBO Rep. *8*, 1080–1085.

Bianchi, A., and Shore, D. (2007). Increased association of telomerase with short telomeres in yeast. Genes Dev. *21*, 1726–1730.

Britt-Compton, B., Capper, R., Rowson, J., and Baird, D.M. (2009). Short telomeres are preferentially elongated by telomerase in human cells. FEBS Lett. *583*, 3076–3080.

Celli, G.B., and de Lange, T. (2005). DNA processing is not required for ATM-mediated telomere damage response after TRF2 deletion. Nat. Cell Biol. *7*, 712–718.

Chan, S.W., Chang, J., Prescott, J., and Blackburn, E.H. (2001). Altering telomere structure allows telomerase to act in yeast lacking ATM kinases. Curr. Biol. *11*, 1240–1250.

Chang, Y.T., Moser, B.A., and Nakamura, T.M. (2013). Fission yeast shelterin regulates DNA polymerases and Rad3(^{ATR}) kinase to limit telomere extension. PLoS Genet. *9*, e1003936.

Churikov, D., Corda, Y., Luciano, P., and Géli, V. (2013). Cdc13 at a crossroads of telomerase action. Front. Oncol. *3*, 39.

Cohen, S.B., and Reddel, R.R. (2008). A sensitive direct human telomerase activity assay. Nat. Methods *5*, 355–360.

Cohen, S.B., Graham, M.E., Lovrecz, G.O., Bache, N., Robinson, P.J., and Reddel, R.R. (2007). Protein composition of catalytically active human telomerase from immortal cells. Science *315*, 1850–1853.

Colgin, L.M., Baran, K., Baumann, P., Cech, T.R., and Reddel, R.R. (2003). Human POT1 facilitates telomere elongation by telomerase. Curr. Biol. *13*, 942–946.

Dalby, A.B., Hofr, C., and Cech, T.R. (2015). Contributions of the TEL-patch amino acid cluster on TPP1 to telomeric DNA synthesis by human telomerase. J. Mol. Biol. *427* (*6 Pt B*), 1291–1303.

de Lange, T. (1992). Human telomeres are attached to the nuclear matrix. EMBO J. *11*, 717–724.

de Lange, T. (2005). Shelterin: the protein complex that shapes and safeguards human telomeres. Genes Dev. *19*, 2100–2110.

Dehé, P.M., Rog, O., Ferreira, M.G., Greenwood, J., and Cooper, J.P. (2012). Taz1 enforces cell-cycle regulation of telomere synthesis. Mol. Cell *46*, 797–808.

Denchi, E.L., and de Lange, T. (2007). Protection of telomeres through independent control of ATM and ATR by TRF2 and POT1. Nature *448*, 1068–1071.

Feldser, D., Strong, M.A., and Greider, C.W. (2006). Ataxia telangiectasia mutated (Atm) is not required for telomerase-mediated elongation of short telomeres. Proc. Natl. Acad. Sci. USA *103*, 2249–2251.

Fokas, E., Prevo, R., Hammond, E.M., Brunner, T.B., McKenna, W.G., and Muschel, R.J. (2014). Targeting ATR in DNA damage response and cancer therapeutics. Cancer Treat. Rev. *40*, 109–117.

Fouché, N., Ozgür, S., Roy, D., and Griffith, J.D. (2006). Replication fork regression in repetitive DNAs. Nucleic Acids Res. *34*, 6044–6050.

Guo, X., Deng, Y., Lin, Y., Cosme-Blanco, W., Chan, S., He, H., Yuan, G., Brown, E.J., and Chang, S. (2007). Dysfunctional telomeres activate an ATM-ATR-dependent DNA damage response to suppress tumorigenesis. EMBO J. *26*, 4709–4719.

Guo, Y., Kartawinata, M., Li, J., Pickett, H.A., Teo, J., Kilo, T., Barbaro, P.M., Keating, B., Chen, Y., Tian, L., et al. (2014). Inherited bone marrow failure associated with germline mutation of *ACD*, the gene encoding telomere protein TPP1. Blood *124*, 2767–2774.

Hector, R.E., Shtofman, R.L., Ray, A., Chen, B.R., Nyun, T., Berkner, K.L., and Runge, K.W. (2007). Tel1p preferentially associates with short telomeres to stimulate their elongation. Mol. Cell *27*, 851–858.

Hemann, M.T., Strong, M.A., Hao, L.Y., and Greider, C.W. (2001). The shortest telomere, not average telomere length, is critical for cell viability and chromosome stability. Cell *107*, 67–77.

Hickson, I., Zhao, Y., Richardson, C.J., Green, S.J., Martin, N.M., Orr, A.I., Reaper, P.M., Jackson, S.P., Curtin, N.J., and Smith, G.C. (2004). Identification and characterization of a novel and specific inhibitor of the ataxia-telangiectasia mutated kinase ATM. Cancer Res. *64*, 9152–9159.

Ivessa, A.S., Zhou, J.Q., Schulz, V.P., Monson, E.K., and Zakian, V.A. (2002). *Saccharomyces* Rrm3p, a 5′ to 3′ DNA helicase that promotes replication fork progression through telomeric and subtelomeric DNA. Genes Dev. *16*, 1383–1396.

Jády, B.E., Richard, P., Bertrand, E., and Kiss, T. (2006). Cell cycle-dependent recruitment of telomerase RNA and Cajal bodies to human telomeres. Mol. Biol. Cell *17*, 944–954.

Jurczyluk, J., Nouwens, A.S., Holien, J.K., Adams, T.E., Lovrecz, G.O., Parker, M.W., Cohen, S.B., and Bryan, T.M. (2011). Direct involvement of the TEN domain at the active site of human telomerase. Nucleic Acids Res. *39*, 1774–1788.

Karlseder, J., Smogorzewska, A., and de Lange, T. (2002). Senescence induced by altered telomere state, not telomere loss. Science *295*, 2446–2449.

Karlseder, J., Hoke, K., Mirzoeva, O.K., Bakkenist, C., Kastan, M.B., Petrini, J.H., and de Lange, T. (2004). The telomeric protein TRF2 binds the ATM kinase and can inhibit the ATM-dependent DNA damage response. PLoS Biol. *2*, E240.

Kelleher, C., Kurth, I., and Lingner, J. (2005). Human protection of telomeres 1 (POT1) is a negative regulator of telomerase activity *in vitro*. Mol. Cell. Biol. *25*, 808–818.

Kim, N.W., Piatyszek, M.A., Prowse, K.R., Harley, C.B., West, M.D., Ho, P.L., Coviello, G.M., Wright, W.E., Weinrich, S.L., and Shay, J.W. (1994). Specific association of human telomerase activity with immortal cells and cancer. Science *266*, 2011–2015.

Kishi, S., Zhou, X.Z., Ziv, Y., Khoo, C., Hill, D.E., Shiloh, Y., and Lu, K.P. (2001). Telomeric protein Pin2/TRF1 as an important ATM target in response to double strand DNA breaks. J. Biol. Chem. *276*, 29282–29291.

Kocak, H., Ballew, B.J., Bisht, K., Eggebeen, R., Hicks, B.D., Suman, S., O'Neil, A., Giri, N., Maillard, I., Alter, B.P., et al.; NCI DCEG Cancer Genomics Research Laboratory; NCI DCEG Cancer Sequencing Working Group (2014). Hoyeraal-Hreidarsson syndrome caused by a germline mutation in the TEL patch of the telomere protein TPP1. Genes Dev. *28*, 2090–2102.

Lee, S.S., Bohrson, C., Pike, A.M., Wheelan, S.J., and Greider, C.W. (2015). ATM kinase is required for telomere elongation in mouse and human cells. Cell Rep. *13*, this issue, 1670–1682.

Lei, M., Zaug, A.J., Podell, E.R., and Cech, T.R. (2005). Switching human telomerase on and off with hPOT1 protein *in vitro*. J. Biol. Chem. *280*, 20449–20456.

Loayza, D., and De Lange, T. (2003). POT1 as a terminal transducer of TRF1 telomere length control. Nature *423*, 1013–1018.

Lovejoy, C.A., and Cortez, D. (2009). Common mechanisms of PIKK regulation. DNA Repair (Amst.) *8*, 1004–1008.

Martínez, P., Thanasoula, M., Muñoz, P., Liao, C., Tejera, A., McNees, C., Flores, J.M., Fernández-Capetillo, O., Tarsounas, M., and Blasco, M.A. (2009). Increased telomere fragility and fusions resulting from TRF1 deficiency lead to degenerative pathologies and increased cancer in mice. Genes Dev. *23*, 2060–2075.

McKerlie, M., Lin, S., and Zhu, X.D. (2012). ATM regulates proteasome-dependent subnuclear localization of TRF1, which is important for telomere maintenance. Nucleic Acids Res. *40*, 3975–3989.

McNees, C.J., Tejera, A.M., Martínez, P., Murga, M., Mulero, F., Fernandez-Capetillo, O., and Blasco, M.A. (2010). ATR suppresses telomere fragility and recombination but is dispensable for elongation of short telomeres by telomerase. J. Cell Biol. *188*, 639–652.

Metcalfe, J.A., Parkhill, J., Campbell, L., Stacey, M., Biggs, P., Byrd, P.J., and Taylor, A.M. (1996). Accelerated telomere shortening in ataxia telangiectasia. Nat. Genet. *13*, 350–353.

Miller, K.M., Rog, O., and Cooper, J.P. (2006). Semi-conservative DNA replication through telomeres requires Taz1. Nature *440*, 824–828.

Moser, B.A., Subramanian, L., Khair, L., Chang, Y.T., and Nakamura, T.M. (2009). Fission yeast Tel1(ATM) and Rad3(ATR) promote telomere protection and telomerase recruitment. PLoS Genet. *5*, e1000622.

Moser, B.A., Chang, Y.T., Kosti, J., and Nakamura, T.M. (2011). $Tel1^{ATM}$ and $Rad3^{ATR}$ kinases promote Ccq1-Est1 interaction to maintain telomeres in fission yeast. Nat. Struct. Mol. Biol. *18*, 1408–1413.

Nandakumar, J., Bell, C.F., Weidenfeld, I., Zaug, A.J., Leinwand, L.A., and Cech, T.R. (2012). The TEL patch of telomere protein TPP1 mediates telomerase recruitment and processivity. Nature *492*, 285–289.

Ohki, R., and Ishikawa, F. (2004). Telomere-bound TRF1 and TRF2 stall the replication fork at telomeric repeats. Nucleic Acids Res. *32*, 1627–1637.

Okamoto, K., Bartocci, C., Ouzounov, I., Diedrich, J.K., Yates, J.R., 3rd, and Denchi, E.L. (2013). A two-step mechanism for TRF2-mediated chromosome-end protection. Nature *494*, 502–505.

Palm, W., and de Lange, T. (2008). How shelterin protects mammalian telomeres. Annu. Rev. Genet. *42*, 301–334.

Pennarun, G., Hoffschir, F., Revaud, D., Granotier, C., Gauthier, L.R., Mailliet, P., Biard, D.S., and Boussin, F.D. (2010). ATR contributes to telomere maintenance in human cells. Nucleic Acids Res. *38*, 2955–2963.

Rog, O., and Cooper, J.P. (2008). Telomeres in drag: Dressing as DNA damage to engage telomerase. Curr. Opin. Genet. Dev. *18*, 212–220.

Sabourin, M., Tuzon, C.T., and Zakian, V.A. (2007). Telomerase and Tel1p preferentially associate with short telomeres in *S. cerevisiae*. Mol. Cell *27*, 550–561.

Sexton, A.N., Regalado, S.G., Lai, C.S., Cost, G.J., O'Neil, C.M., Urnov, F.D., Gregory, P.D., Jaenisch, R., Collins, K., and Hockemeyer, D. (2014). Genetic and molecular identification of three human TPP1 functions in telomerase

action: recruitment, activation, and homeostasis set point regulation. Genes Dev. *28*, 1885–1899.

Sfeir, A., Kosiyatrakul, S.T., Hockemeyer, D., MacRae, S.L., Karlseder, J., Schildkraut, C.L., and de Lange, T. (2009). Mammalian telomeres resemble fragile sites and require TRF1 for efficient replication. Cell *138*, 90–103.

Shay, J.W., and Bacchetti, S. (1997). A survey of telomerase activity in human cancer. Eur. J. Cancer *33*, 787–791.

Smilenov, L.B., Morgan, S.E., Mellado, W., Sawant, S.G., Kastan, M.B., and Pandita, T.K. (1997). Influence of ATM function on telomere metabolism. Oncogene *15*, 2659–2665.

Smogorzewska, A., van Steensel, B., Bianchi, A., Oelmann, S., Schaefer, M.R., Schnapp, G., and de Lange, T. (2000). Control of human telomere length by TRF1 and TRF2. Mol. Cell. Biol. *20*, 1659–1668.

Sprung, C.N., Bryan, T.M., Reddel, R.R., and Murnane, J.P. (1997). Normal telomere maintenance in immortal ataxia telangiectasia cell lines. Mutat. Res. *379*, 177–184.

Stern, J.L., and Bryan, T.M. (2008). Telomerase recruitment to telomeres. Cytogenet. Genome Res. *122*, 243–254.

Stern, J.L., Zyner, K.G., Pickett, H.A., Cohen, S.B., and Bryan, T.M. (2012). Telomerase recruitment requires both TCAB1 and Cajal bodies independently. Mol. Cell. Biol. *32*, 2384–2395.

Stiff, T., Walker, S.A., Cerosaletti, K., Goodarzi, A.A., Petermann, E., Concannon, P., O'Driscoll, M., and Jeggo, P.A. (2006). ATR-dependent phosphorylation and activation of ATM in response to UV treatment or replication fork stalling. EMBO J. *25*, 5775–5782.

Takai, K.K., Hooper, S., Blackwood, S., Gandhi, R., and de Lange, T. (2010). *In vivo* stoichiometry of shelterin components. J. Biol. Chem. *285*, 1457–1467.

Teixeira, M.T., Arneric, M., Sperisen, P., and Lingner, J. (2004). Telomere length homeostasis is achieved via a switch between telomerase- extendible and -nonextendible states. Cell *117*, 323–335.

Tomlinson, R.L., Ziegler, T.D., Supakorndej, T., Terns, R.M., and Terns, M.P. (2006). Cell cycle-regulated trafficking of human telomerase to telomeres. Mol. Biol. Cell *17*, 955–965.

Tomlinson, R.L., Abreu, E.B., Ziegler, T., Ly, H., Counter, C.M., Terns, R.M., and Terns, M.P. (2008). Telomerase reverse transcriptase is required for the localization of telomerase RNA to cajal bodies and telomeres in human cancer cells. Mol. Biol. Cell *19*, 3793–3800.

Tomlinson, C.G., Moye, A.L., Holien, J.K., Parker, M.W., Cohen, S.B., and Bryan, T.M. (2015). Two-step mechanism involving active-site conformational changes regulates human telomerase DNA binding. Biochem. J. *465*, 347–357.

van Steensel, B., and de Lange, T. (1997). Control of telomere length by the human telomeric protein TRF1. Nature *385*, 740–743.

Veldman, T., Etheridge, K.T., and Counter, C.M. (2004). Loss of hPot1 function leads to telomere instability and a cut-like phenotype. Curr. Biol. *14*, 2264–2270.

Verdun, R.E., and Karlseder, J. (2006). The DNA damage machinery and homologous recombination pathway act consecutively to protect human telomeres. Cell *127*, 709–720.

Wang, F., Podell, E.R., Zaug, A.J., Yang, Y., Baciu, P., Cech, T.R., and Lei, M. (2007). The POT1-TPP1 telomere complex is a telomerase processivity factor. Nature *445*, 506–510.

Wenz, C., Enenkel, B., Amacker, M., Kelleher, C., Damm, K., and Lingner, J. (2001). Human telomerase contains two cooperating telomerase RNA molecules. EMBO J. *20*, 3526–3534.

Wong, K.K., Maser, R.S., Bachoo, R.M., Menon, J., Carrasco, D.R., Gu, Y., Alt, F.W., and DePinho, R.A. (2003). Telomere dysfunction and Atm deficiency compromises organ homeostasis and accelerates ageing. Nature *421*, 643–648.

Wu, Y., Xiao, S., and Zhu, X.D. (2007). MRE11-RAD50-NBS1 and ATM function as co-mediators of TRF1 in telomere length control. Nat. Struct. Mol. Biol. *14*, 832–840.

Yamazaki, H., Tarumoto, Y., and Ishikawa, F. (2012). Tel1(^{ATM}) and Rad3(^{ATR}) phosphorylate the telomere protein Ccq1 to recruit telomerase and elongate telomeres in fission yeast. Genes Dev. *26*, 241–246.

Ye, J.Z., Hockemeyer, D., Krutchinsky, A.N., Loayza, D., Hooper, S.M., Chait, B.T., and de Lange, T. (2004). POT1-interacting protein PIP1: a telomere length regulator that recruits POT1 to the TIN2/TRF1 complex. Genes Dev. *18*, 1649–1654.

Zaug, A.J., Podell, E.R., and Cech, T.R. (2005). Human POT1 disrupts telomeric G-quadruplexes allowing telomerase extension *in vitro*. Proc. Natl. Acad. Sci. USA *102*, 10864–10869.

Zhong, F.L., Batista, L.F., Freund, A., Pech, M.F., Venteicher, A.S., and Artandi, S.E. (2012). TPP1 OB-fold domain controls telomere maintenance by recruiting telomerase to chromosome ends. Cell *150*, 481–494.

Zimmermann, M., Kibe, T., Kabir, S., and de Lange, T. (2014). TRF1 negotiates TTAGGG repeat-associated replication problems by recruiting the BLM helicase and the TPP1/POT1 repressor of ATR signaling. Genes Dev. *28*, 2477–2491.

Cell Reports

Supplemental Information

ATM and ATR Signaling Regulate the Recruitment of Human Telomerase to Telomeres

Adrian S. Tong, J. Lewis Stern, Agnel Sfeir, Melissa Kartawinata, Titia de Lange, Xu-Dong Zhu, and Tracy M. Bryan

Figure S1. Related to Figure 1.

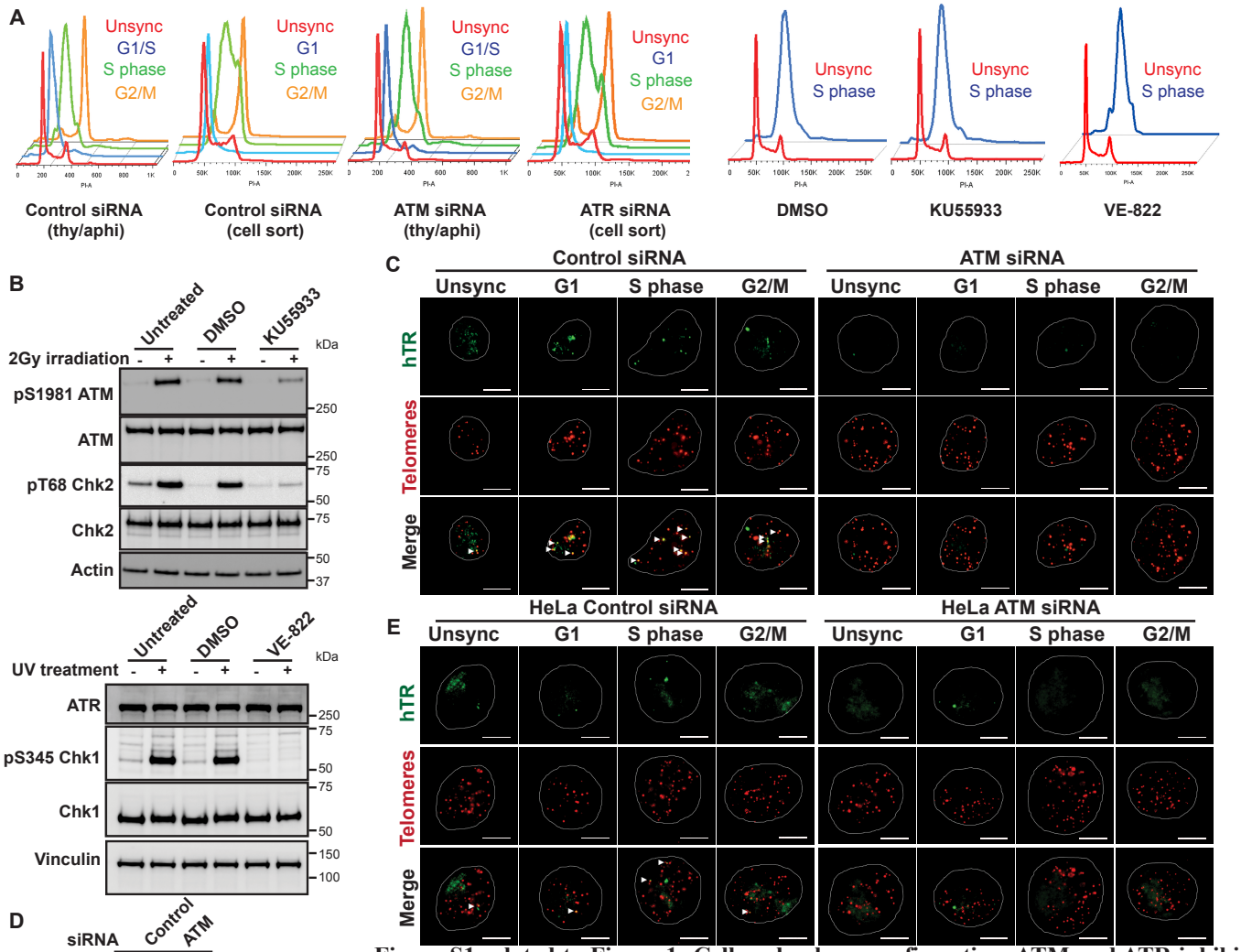

Figure S1 related to Figure 1: Cell cycle phase confirmation, ATM and ATR inhibition controls, and telomerase recruitment after ATM siRNA in HeLa cells.

(A) Cell cycle analysis by flow cytometry of propidium iodide-stained 293T cells treated with control siRNA, ATM siRNA, DMSO control, 1.5 μM ATM inhibitor KU-55933 or 500 nM ATR inhibitor VE-822.

(B) Immunoblots for 293T cells treated with DMSO control, 1.5 μM ATM inhibitor KU-55933 or 500 nM ATR inhibitor VE-822 in the presence or absence of 2 Gy γ-irradiation or 2 mW of ultraviolet treatment, respectively, probed with the indicated antibodies to observe activation of ATM or ATR and their substrates Chk2 or Chk1; actin and vinculin were probed as controls.

(C) hTR/telomere FISH in 293T cells treated with control or ATM siRNA and synchronized with thymidine/aphidicolin. White arrows indicate hTR signals co-localizing with telomeric signals, scale bar = 10 μm.

(D) Immunoblot of HeLa cells treated with control or ATM siRNA and probed for ATM knockdown, with actin as a control.

(E) hTR/telomere FISH in HeLa cells treated with control or ATM siRNA and synchronized with a double thymidine block. White arrows indicate hTR signals co-localizing with telomeric signals, scale bar = 10 μm.

(F) Quantitation of average (± SD) co-localizations between hTR and telomeric signals in asynchronous HeLa cells following control (black) or ATM (red) siRNA treatment; n =3.

(G) Average telomerase recruitment over the cell cycle (± SD) in HeLa cells treated with control (black) or ATM (red) siRNA. Cells were sorted by FACS into the indicated cell cycle phases; n = 3.

Figure S2. Related to Figure 2.

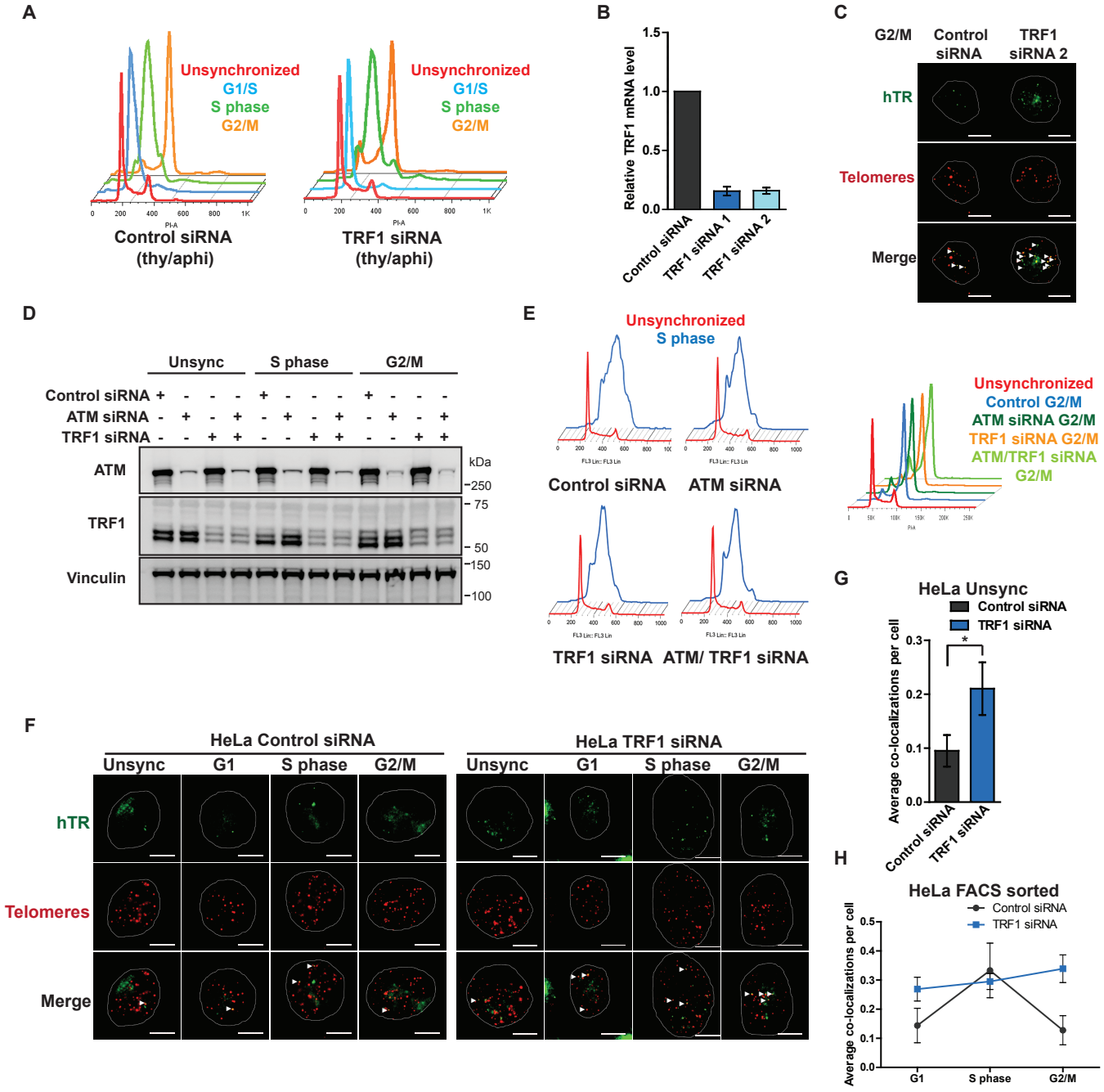

Figure S2 related to Figure 2: Cell cycle phase confirmation, TRF1 and ATM silencing controls, and telomerase recruitment after TRF1 siRNA in HeLa cells.

(A) Cell cycle analysis by flow cytometry of propidium iodide-stained 293T cells treated with TRF1 or control siRNA.
(B) Quantitation of TRF1 mRNA levels using qRT-PCR after TRF1 knockdown in 293T cells.
(C) hTR/telomere FISH in thymidine/aphidicolin synchronized 293T cells treated with TRF1 siRNA, and harvested at G2/M phase; scale bar = 10 μm.
(D) Immunoblots for ATM and TRF1 in 293T cells treated with control, ATM only, TRF1 only or double ATM/TRF1 siRNA, with vinculin probed as a control.
(E) Cell cycle analysis by flow cytometry of propidium iodide-stained 293T cells treated as in Figure S2D.
(F) hTR/telomere FISH in HeLa cells treated with control or TRF1 siRNA and sorted by FACS into the indicated cell cycle phases. White arrows indicate hTR signals co-localizing with telomeric signals; scale bar = 10 μm.
(G) Quantitation of average co-localization between hTR and telomeric signals in asynchronous HeLa cells following control (black) or TRF1 (blue) siRNA treatment; *p = 0.0103.
(H) Average telomerase recruitment over the cell cycle in HeLa cells treated with control (black) or TRF1 (blue) siRNA. Cells were sorted by FACS into the indicated cell cycle phases.

In all panels, data is presented as the mean of three independent experiments, and error bars indicate standard deviation.

Figure S3 related to Figure 3: Controls and extra images for experiments involving overexpression of myc-TRF1.

(A) Relative total TRF1 mRNA abundance measured by qRT-PCR in 293T cells overexpressing WT, S367A, S367D myc-tagged TRF1.

(B) Profile of Vybrant DyeCycle Violet-stained 293T cells as seen in the cell sorter, illustrating the gating used to isolate cells in G1, mid-S and G2/M phases of the cell cycle in experiment in Figure S3C.

(C) Anti-myc immunofluorescence and hTR/telomere FISH in 293T cells overexpressing WT, S367A, and S367D myc-tagged TRF1. White arrows represent co-localizations between myc-TRF1 and telomeres, yellow arrows represent co-localizations between hTR and telomeres while green arrows represent tri-localizations. Scale bar = 10 µm.

(D) Average telomerase recruitment over the cell cycle (± SD) in HeLa cells stably overexpressing vector control (black), shRNA against TRF1 (grey), WT TRF1 (blue), S367A TRF1 (green) and S367D TRF1 (pink). The latter 3 cell lines expressed both TRF1 shRNA and an shRNA-resistant TRF1 construct. Cells were synchronized by a double thymidine block into the indicated cell cycle phases; *p < 0.05, **p < 0.01, n = 3 - 4.

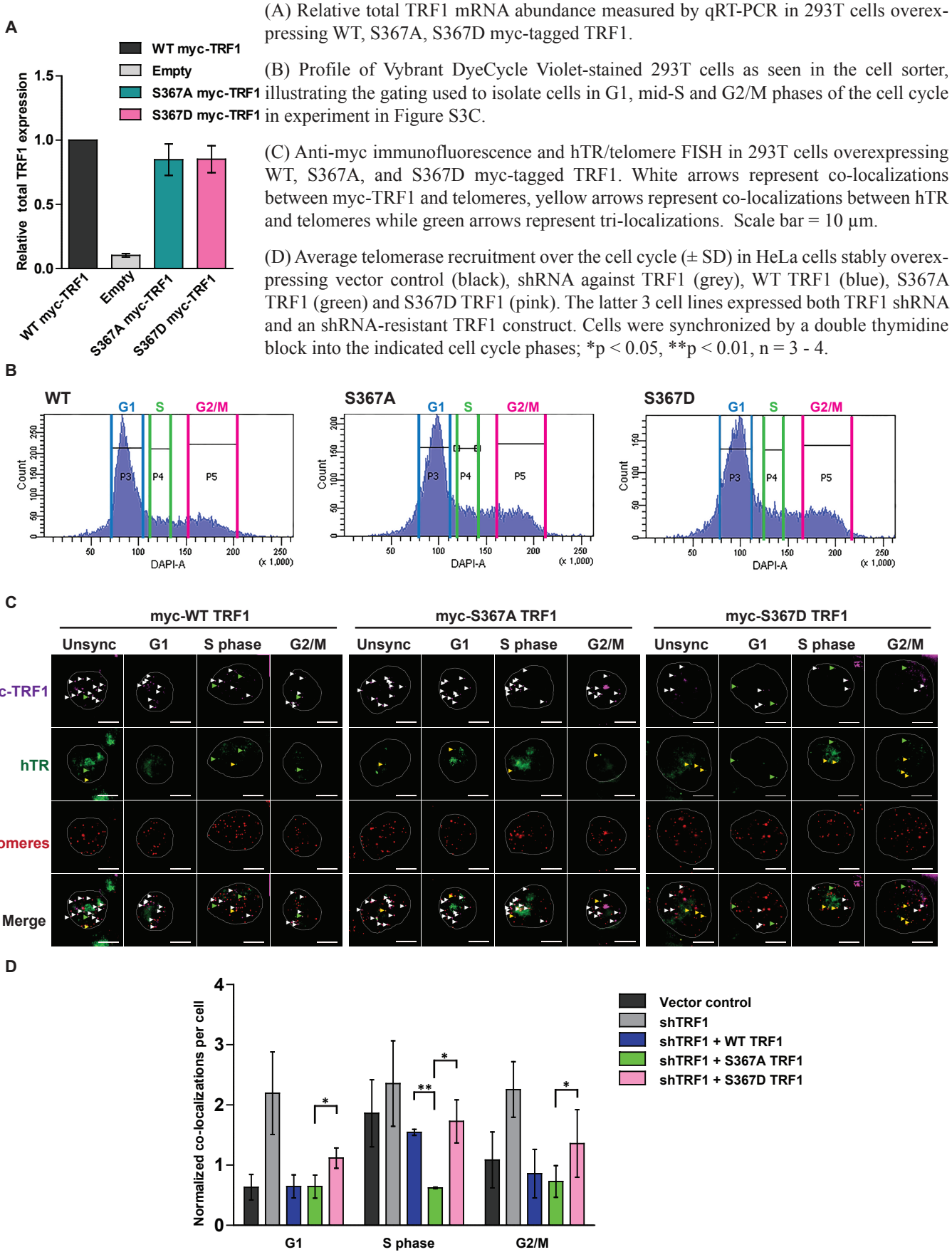

Figure S4. Related to Figure 4.

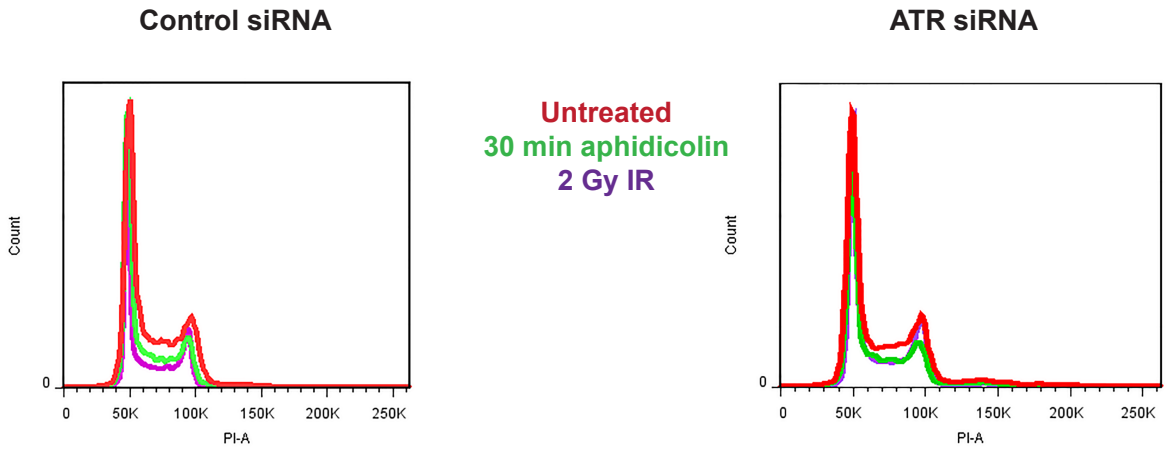

Figure S4 related to Figure 4: Cell cycle phase confirmation after DNA damage treatments

Cell cycle analysis by flow cytometry of propidium iodide-stained 293T cells treated with control or ATR siRNA and the indicated treatments, to ensure that the induction of DNA damage did not alter the cell cycle profile.

Figure S5. Related to Figure 6.

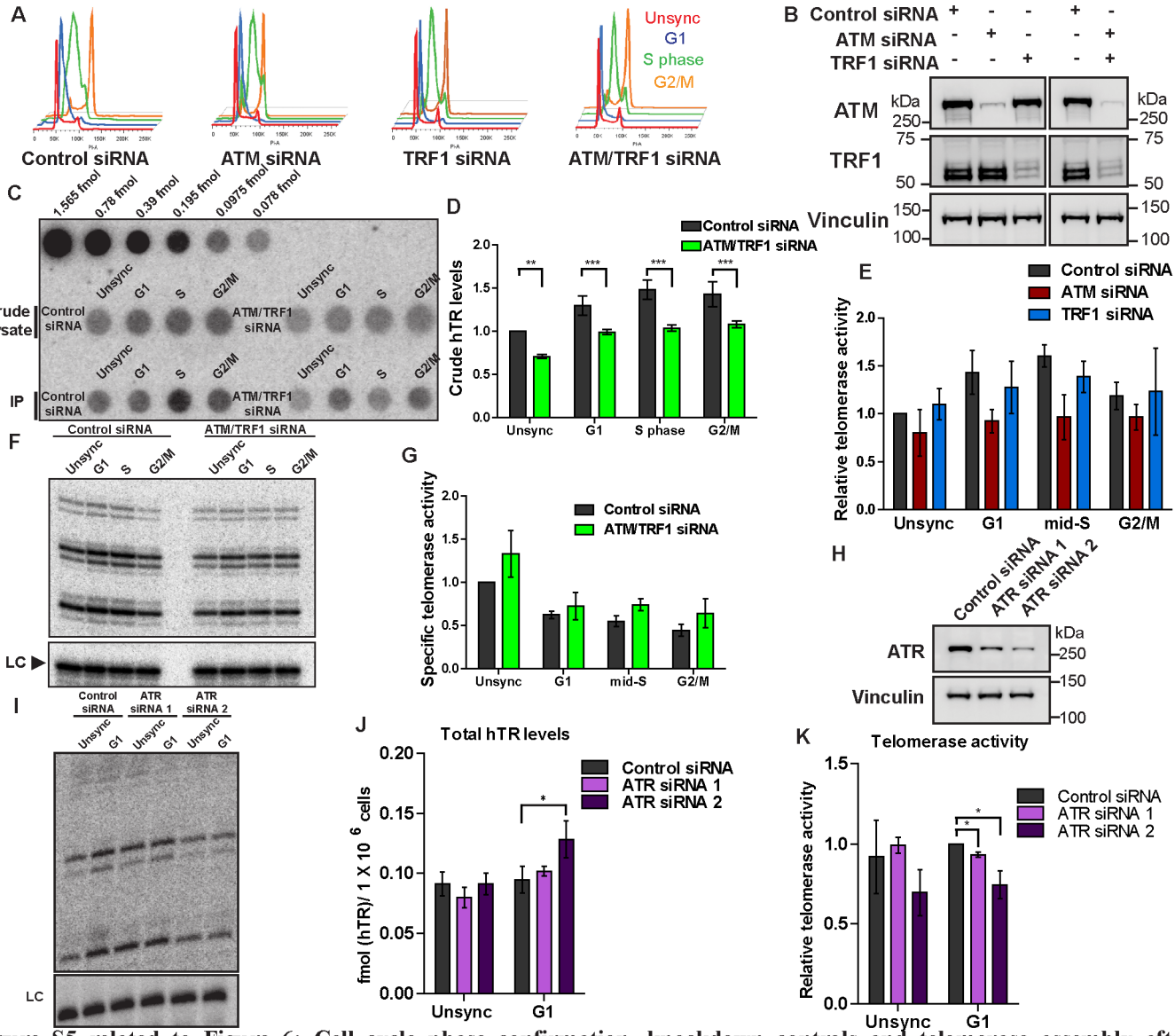

Figure S5 related to Figure 6: Cell cycle phase confirmation, knockdown controls and telomerase assembly after ATM/TRF1 double knockdown and ATR knockdown.

(A) Cell cycle analysis by flow cytometry of propidium iodide-stained 293T cells treated with control, ATM only, TRF1 only and ATM/TRF1 double siRNA for telomerase hTR dot blot and telomerase activity experiments (Figure 6).

(B) Immunoblot to determine ATM and TRF1 abundance in 293T cells after treatment with control, ATM only, TRF1 only and ATM/ TRF1 double siRNA. Vinculin was probed as a control.

(C) Dot blot for hTR in 293T cells treated with control or ATM/TRF1 siRNA before and after immunoprecipitation with hTERT antibody. Crude cell lysates (top panel) contain total levels of cellular hTR while hTERT immunoprecipitated samples (IP) contain only hTR that has assembled with hTERT. Top row: in vitro-transcribed hTR standard.

(D) Quantitation of dot blot for hTR in 293T cells in Supplemental Figure 5 C. Total levels of hTR in control (black) and ATM/TRF1 (green) siRNA cells were quantitated using the hTR standard; **$p < 0.01$, ***$p < 0.005$.

(E) Relative telomerase activity levels from Figure 6E, normalised to cell number and loading control, but not normalized to levels of hTR recovered.

(F) Direct telomerase activity assay of immunoprecipitated telomerase from 293T cells treated with control or ATM/TRF1 siRNA. LC represents an 18 nt loading control.

(G) Quantitation of specific activity of telomerase treated with contol (black) or ATM/TRF1 (green) siRNA cells. Levels of relative specific telomerase activity were derived from total telomerase activity normalized to levels of hTR after hTERT immuno-precipitation (Figure 6D).

(H) Immunoblot to determine ATR abundance in 293T cells after ATR knockdown. Vinculin was probed as a control.

(I) Direct telomerase activity assay of immunoprecipitated telomerase from 293T cells treated with control or ATR siRNA. LC represents an 18 nt loading control.

(J) Quantitation of total hTR levels after ATR siRNA; *$p < 0.05$.

(K) Relative telomerase activity levels from supp Figure 5I, normalized to cell number and loading control, but not normalized to levels of hTR recovered; *$p < 0.05$.

In all panels, data is presented as the mean of three independent experiments, and error bars indicate standard deviation.

Supplemental Table S1. Related to Figures 1-4, 6.

Protein Name	siRNA	Company	Catalogue number	Sequence (5'- 3')
ATR	Hs_ATR 11 Flexi Tube	QIAGEN	SI02660231	5'-AAGGACATGTGCATTACCTTA-3'
ATR	Hs_ATR 12 Flexi Tube	QIAGEN	SI02664347	5'-CAGGCACTAATTGTTCTTCAA-3'
ATM	Hs_ATM_5 Flexi Tube	QIAGEN	SI00299299	5'-AAGGCTATTCAGTGTGCGAGA-3'
ATM	ATM stealth siRNA	Invitrogen	HSS181473	
TRF1	TRF1 siRNA	QIAGEN (custom)	1027423	5'-AAGAATATTTGGTGATCCAAA-3'
TRF1	Hs_TERF1_10 GeneSolution	QIAGEN	SI04906062	5'-TTGCCAGTTGAGAACGATATA-3'
Control	All Stars Negative control	QIAGEN	1027281	